UCLA-ENG-7382
FEBRUARY 1974

TRANSONIC CONICAL FLOW

K.G. AGOPIAN

UCLA • SCHOOL OF ENGINEERING AND APPLIED SCIENCE

TRANSONIC CONICAL FLOW

by

Kaloust Gregory Agopian

SCHOOL OF ENGINEERING AND APPLIED SCIENCE
UNIVERSITY OF CALIFORNIA
LOS ANGELES, CALIFORNIA

Page Intentionally Left Blank

ACKNOWLEDGMENTS

Page Intentionally Left Blank

ABSTRACT

The problem of inviscid, steady transonic conical flow formulated in terms of the small disturbance theory is studied. The small disturbance equation and similarity rules are presented, and a boundary value problem is formulated for the case of a supersonic freestream Mach number. The equation for the perturbation potential is solved numerically using an elliptic finite difference system. The difference equations are solved with a point relaxation algorithm that is also capable of capturing the shock wave during the iteration procedure by using the boundary conditions at the shock. Numerical calculations, for shock location, pressure distribution and drag coefficient, are presented for a family of nonlifting conical wings.

The theory of slender wings is also presented and analytical results for pressure and drag coefficients are obtained.

Page Intentionally Left Blank

TABLE OF CONTENTS

SYMBOLS

a	speed of sound
a_1, a_2, a_3, a_4	transonic equation coefficients
b	wing halfspan
B	wing similarity parameter
C_1	slender wing similarity parameter
C_D	drag coefficient
C_P	pressure coefficient
D	$a_2^2 - a_1 a_3$
E	longitudinal cross-sectional area distribution
f	wing shape function
F	wing shape function in conical variables
g	shock wave shape function
G	$x - g$
$\vec{i}$, $\vec{j}$, $\vec{k}$	unit vectors in the x, y, z directions respectively
J	Jacobian
k	proportionality constant
K	transonic similarity parameter
K_e	transonic similarity parameter for axisymmetric flow
M	Mach number
$\vec{n}$	unit normal to the shock wave surface
p	perturbation pressure
PC	$\phi_\xi(\xi = 0)$
PCA	$\phi_{\xi\eta}(\xi = 0)$
$\vec{q}$	velocity vector
R_{MC}	initial shock wave location

S	$y - \delta f$
U	freestream magnitude of $\vec{q}$
u, v, w	perturbation velocity components in the x, y, z directions respectively
x, y, z	cartesian coordinates
x, $\tilde{y}$, $\tilde{z}$	transonic coordinates
Y, Z	transonic conical coordinates
γ	ratio of specific heats
2δ	thickness of wing at x = 1
δ_e	equivalent body of revolution radius at x = 1
ξ, η	transonic conical elliptic cylinder coordinates
ρ	density
Φ	exact potential
φ	perturbation potential
ϕ	conical perturbation potential
ω	relaxation parameter

Subscripts

i,j	mesh point indices in the ξ and η directions, respectively
∞	freestream conditions

Superscripts

*	outer expansion variable
—	inner expansion variable

CHAPTER 1

INTRODUCTION

Transonic flows are characterized by the presence of a region where the local flow speed is close to the local speed of sound. In flows of this nature shock waves are generally present in the supersonic region or at the downstream supersonic-subsonic interface. Mathematically this problem is described by a nonlinear equation which is elliptic if the flow is subsonic or hyperbolic if the flow is supersonic.

Intense theoretical and experimental work started in the late forties and resulted in a good understanding of the physical phenomenon. Newman and Allison[1] give a listing of over 300 theoretical papers and Cole[2] gives a brief historical survey leading to problems of current interest. Those problems are of great engineering interest because they occur in a number of practical situations such as flows in nozzles, over helicopter rotors, propellers and over airplanes flying close to Mach number one.

The method of the hodograph transformation, which makes the equation linear, was the first to yield quantitative information about transonic flows over two dimensional bodies. The hodograph method is useful in the case of the straight wedge and can also yield a solution valid in the vicinity of blunt noses. However, its applicability is hindered since boundary conditions, inherently given in the physical plane, usually become very complicated in the hodograph plane. The limitation is thus in solving direct problems. Garabedian and Korn[3] have found this method useful in computing the inverse problem; the airfoil for a given flow field.

In computing solutions successfully over arbitrary planar shapes two basic approaches have been used. Both approaches, the time dependent techniques and the relaxation methods use finite difference techniques and are capable of capturing imbedded shocks. The time dependent technique (Magnus and Yoshihara)[4] integrates the equations of unsteady compressible flow forward in time to approach a steady state. This method is quite lengthy for general application. A simpler and faster method for symmetric bodies was first developed by Murman and Cole[5] who solved the transonic small disturbance equation for the potential. Subsequent work (Krupp and Murman,[6] Krupp[7]) improved this procedure and extended it to lifting airfoils. The results have been shown to give remarkably good results.

For three-dimensional transonic flows only a few solutions are available thus far. One due to Ballhaus and Bailey,[8] extends the relaxation procedure of Murman and Cole to solve three-dimensional supercritical flows over lifting wings with blunt leading edges and non-rectangular planforms. However, the solutions available are all for subsonic freestream Mach numbers.

The purpose of this dissertation is to develop on effective numerical method for computing three-dimensional transonic flows with "supersonic" conditions. More specifically nonlifting conical wings with the shock attached to the nose of the wing will be considered.

This dissertation will be presented in three major parts, consisting of Chapters 2, 3 and 4. Chapter 2 formulates the boundary value problem and gives the basic analytic results needed for the numerical

computation. Chapter 3 discusses the details of the numerical

computation and presents the results. Chapter 4 presents the slender-

wing theory and compares the results.

Page Intentionally Left Blank

CHAPTER 2

FORMULATION OF GOVERNING EQUATIONS

2.1 BASIC EQUATIONS

The basic differential equations are statements concerning the conservation of mass, momentum and energy for a fluid, plus an equation of state. Since shock waves are present shock jump conditions must be added. The shock jump conditions are integral forms of the above conservation laws. Boundary conditions prescribe the flow at upstream infinity and require the flow to be tangent to the body surface.

The continuity and momentum equations are as follows:

$$\nabla \cdot \rho \vec{q} = 0 \qquad (2.1)$$

$$\vec{q} \cdot \nabla \vec{q} + \frac{1}{\rho} \nabla p = 0 \qquad (2.2)$$

where ρ is the density, $\vec{q}$ the velocity vector and p the pressure; the space coordinates used being non-dimensional.

The energy equation expresses the fact that total enthalpy is conserved along streamlines and it can be shown that it does not jump across a shock surface. Assuming the perfect gas law we can write the energy equation as,

$$\frac{q^2}{2} + \frac{a^2}{\gamma-1} = \frac{U^2}{2} + \frac{a_\infty^2}{\gamma-1} \qquad (2.3)$$

where a = local speed of sound = $\sqrt{\left(\frac{\partial p}{\partial \rho}\right)_S} = \sqrt{\gamma RT}$

$\gamma = \dfrac{C_p}{C_V}$ = constant

U = magnitude of the velocity vector at upstream infinity

a_∞ = speed of sound at upstream infinity.

The only mechanism for entropy production and for introduction of rotation in this inviscid model is a shock wave. The entropy, though constant along streamlines, does jump across a shock wave. It can be proved that the jump in entropy is of a higher order than the equation to be considered.[9] Hence the flow can be assumed isentropic and irrotational.

Using the relation between the speed of sound and the pressure we can rewrite the momentum equation as:

$$\vec{q} \cdot \nabla \vec{q} = -\frac{1}{\rho} \nabla p = -\frac{1}{\rho} \left(\frac{dp}{d\rho}\right) \nabla \rho = -\frac{a^2}{\rho} \nabla \rho \tag{2.4}$$

The continuity equation gives a relation between the density and the velocity of the fluid

$$\nabla \cdot \rho \vec{q} = \vec{q} \cdot \nabla \rho + \rho \nabla \cdot \vec{q} = 0 \tag{2.5}$$

and multiplying the momentum equation (2.4) by $\vec{q}$ enables ρ to be eliminated using the continuity equation (2.5), giving:

$$\vec{q} \cdot \nabla \frac{q^2}{2} = a^2 \nabla \cdot \vec{q} \tag{2.6}$$

Introducing the condition for irrotationality

$$\nabla \times \vec{q} = 0 \tag{2.7}$$

a velocity potential $\Phi(x, y, z)$ can be defined by the relation

$$\vec{q} = \nabla \Phi \tag{2.8}$$

The components of velocity, in equation (2.6), can be substituted by the appropriate partial derivatives of the velocity potential giving a scalar equation for the velocity potential.

$$\left(a^2 - \Phi_x^2\right)\Phi_{xx} + \left(a^2 - \Phi_y^2\right)\Phi_{yy} + \left(a^2 - \Phi_z^2\right)\Phi_{zz}$$

$$-2\Phi_x \Phi_y \Phi_{xy} - 2\Phi_x \Phi_z \Phi_{xz} - 2\Phi_y \Phi_z \Phi_{yz} = 0 \tag{2.9}$$

If the flow at upstream infinity is uniform with magnitude U and parallel to the x axis

$\Phi(x, y, z) = Ux$ at upstream infinity   (2.10)

On the surface of the body the flow must be tangent to the solid surface. This can be expressed as

$\vec{q} \cdot \nabla S = 0$ (2.11)

where $S(x, y, z)$ describes the body surface.

The equation for the potential, together with the above boundary conditions form the basic system describing the flow field.

2.2 DERIVATION OF THE TRANSONIC SMALL DISTURBANCE EQUATION

The solution of equation (2.9) gives the exact flow, with the assumptions outlined in the preceding section. However, there are no practical methods available to solve this equation. We must then look for a simpler equation capable of preserving the features of the exact equation and which could be solved practically.

The equation can be simplified by introducing small disturbance approximations corresponding to flow over thin bodies of thickness 2δ ($\delta \ll 1$).

The small disturbance approximation corresponds to an expansion procedure, for the velocity potential, valid as certain small parameters approach zero.

A special procedure is necessary to derive a suitable small-disturbance approximation when the flow is transonic as opposed to the usual linearized theory.[10] Linearized theory, which has a singularity at $M_\infty = 1$, cannot be used in the transonic range since the solution it

7

gives for the streamwise velocity perturbation becomes infinite as the upstream Mach number approaches one. This violates the assumption of small disturbance.

In the transonic range the expansion should also be asymptotic as the upstream Mach number approaches one, and it will be shown that the quantities δ and $M_\infty^2 - 1$ should not go to zero independently.

The expansion for three dimensional wings of halfspan b and thickness 2δ(Figure 2.1) has the form:

$$\Phi(x,y,z;\ M_\infty,\delta) = U \left\{ x + \varepsilon_1(\delta)\varphi_1(x,\tilde{y},\tilde{z}) + \varepsilon_2(\delta)\varphi_2(x,\tilde{y},\tilde{z}) + \ldots \right\}$$

$$\tilde{y} = \beta(\delta)y \qquad\qquad (2.12)$$

$$\tilde{z} = \beta(\delta)z$$

Linearized theory, where $\beta(\delta) = 1$, fails badly near $M_\infty = 1$ because the orders of certain terms were estimated incorrectly. In order to arrive at the correct expansion let us set $M_\infty = 1$. If a suitable expansion can be obtained for $M_\infty = 1$ then it can be extended in the neighborhood of $M_\infty = 1$ by considering that $M_\infty \to 1$ at a certain rate as $\delta \to 0$.

For $M_\infty = 1$ this limit process cannot be carried out in the original system of coordinates, since this gives the same result as in linearized theory. Instead rescaled $\tilde{y}$ and $\tilde{z}$ coordinates are used. Linearized theory indicates correctly that disturbances spread more rapidly in the transverse direction of flow hence we can expect $\beta(\delta) \to 0$ as $M_\infty \to 1$.

Keeping only the first correction term to the potential and dropping the subscript 1
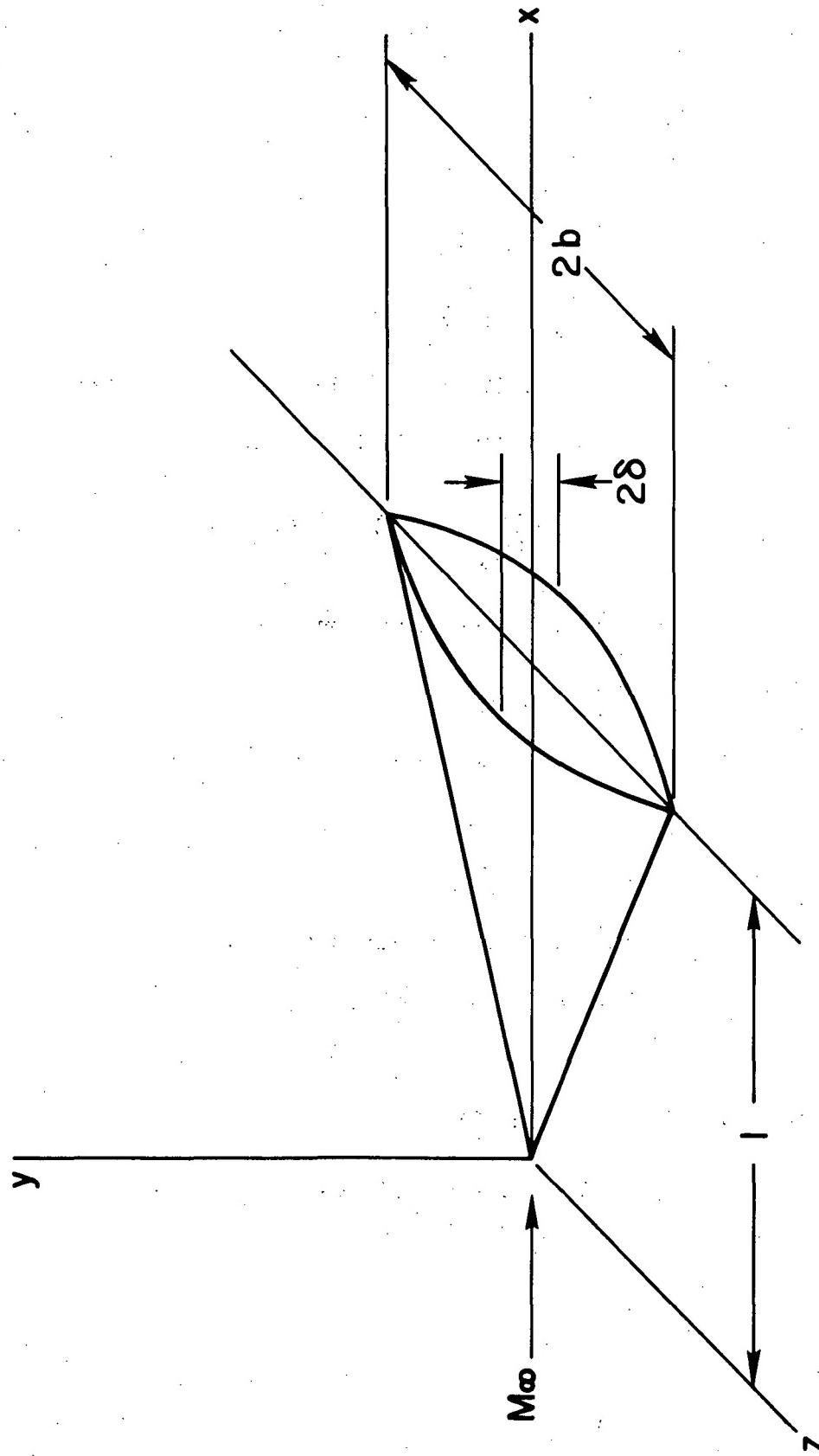
Figure 2.1. Wing Geometry.

$$\Phi_x = U\{1 + \varepsilon\varphi_{\tilde{x}}\} \qquad (2.13)$$

$$\Phi_y = U \varepsilon \beta \varphi_{\tilde{y}} \qquad (2.14)$$

$$\Phi_z = U \varepsilon \beta \varphi_{\tilde{z}} \qquad (2.15)$$

and the energy equation takes the form

$$a^2 = a_\infty^2 - (\gamma-1)U^2\varepsilon\varphi_x + 0(\varepsilon^2) \qquad (2.16)$$

Substituting equations (2.13) - (2.16) in equation (2.9), dividing by U^2 and omitting terms of order ε^2, we obtain

$$\left\{\frac{1}{M_\infty^2} - 1 - (\gamma+1)\varepsilon\varphi_x\right\} \varepsilon\varphi_{xx} + \left\{\frac{1}{M_\infty^2} - (\gamma-1)\varepsilon\varphi_x\right\} (\varphi_{\tilde{y}\tilde{y}} + \varphi_{\tilde{z}\tilde{z}})\varepsilon\beta^2 = 0 \quad (2.17)$$

If we now set $M_\infty = 1$ in the above equation

$$(\gamma+1)\varepsilon^2\varphi_x\varphi_{xx} = \varepsilon\beta^2(\varphi_{\tilde{y}\tilde{y}} + \varphi_{\tilde{z}\tilde{z}})$$

The distinguished limit occurs if $\beta \to 0$ as $\varepsilon \to 0$, in such a way that

$$\varepsilon\beta^2 = \varepsilon^2 \qquad \text{or} \qquad \beta = \sqrt{\varepsilon} \qquad (2.18)$$

The condition that the flow is tangent to the solid surface, equation (2.11), fixes the orders of magnitude of β and ε.
The wing is described by

$$S(x,y,z) = 0 = y - \delta f\left(x, \frac{z}{b}\right) \qquad (2.19)$$

and using equation (2.11) gives the boundary condition for the perturbation potential on the body.

$$\varepsilon\beta\varphi_{\tilde{y}}(x,0,\tilde{z}) = \delta f_x\left(x, \frac{z}{b}\right) \qquad (2.20)$$

10

A comparison of equations (2.18) and (2.20) shows that

$$\varepsilon = \delta^{2/3} \tag{2.21}$$

$$\beta = \delta^{1/3} \tag{2.22}$$

for the distinguished limit. This gives the equation for sonic flow

$$(\gamma+1)\varphi_x \varphi_{xx} = \varphi_{\tilde{y}\tilde{y}} + \phi_{\tilde{z}\tilde{z}} \qquad M_\infty = 1 \tag{2.23}$$

The concept of the limit process leading to the expansion must now be widened to consider $M_\infty \rightarrow 1$ as $\delta \rightarrow 0$, this can be expressed as

$$M_\infty^2 = 1 + K\nu(\delta), \qquad \nu(\delta) \rightarrow 0$$

The quantity K is held fixed in the limit and an order must be found for the function $\nu(\delta)$. To do this we go back to equation (2.17) rearrange it and substitute $K\nu(\delta)$ for $M_\infty^2 - 1$. The distinguished limit exists if

$$\nu(\delta) = \delta^{2/3} \tag{2.24}$$

and results in the transonic equation.

$$\left[K + (\gamma+1)\varphi_x\right] \varphi_{xx} = \varphi_{\tilde{y}\tilde{y}} + \varphi_{\tilde{z}\tilde{z}} \tag{2.25}$$

$$K = \frac{M_\infty^2 - 1}{\delta^{2/3}} \qquad \text{(the transonic similarity parameter)} \tag{2.26}$$

The boundary condition on the wing reduces to

$$\varphi_{\tilde{y}}(x,0,\tilde{z}) = f_x\left(x, \frac{\tilde{z}}{b\delta^{1/3}}\right) \tag{2.27}$$

To make the system describing the flow field a complete one we must next consider the shock jump conditions. These relations can be derived from the surface integral form of equation (2.25) applied across the shock surface plus the requirement that the resultant jump

11

in velocity is normal to the shock surface. Using velocity components u, v and w to substitute for φ_x, $\varphi_{\tilde{y}}$ and $\varphi_{\tilde{z}}$ equation (2.25) can be written in divergence form.

$$\left(-Ku - \frac{\gamma+1}{2}u^2\right)_x + v_{\tilde{y}} + w_{\tilde{z}} = 0 \tag{2.28}$$

The above equation can be interpreted as the transonic continuity equation since it represents the divergence of the mass flux vector. With

$$\vec{Q} = \left(-Ku - \frac{\gamma+1}{2}u^2\right)\vec{i} + v\vec{j} + w\vec{k}$$

(i,j,k are the unit vectors in the x, y and z direction respectively) equation (2.28) can be written as

$$\nabla \cdot \vec{Q} = 0$$

Across the shock surface, Figure 2.2, the jump in the normal component of $\vec{Q}$ is zero and so is the jump in the tangential component of velocity. To incorporate these in equation (2.28) let the shock surface be given by

$$G(x, \tilde{y}, \tilde{z}) = 0 = x - g(\tilde{y}, \tilde{z}) \tag{2.29}$$

Then the unit normal to the shock surface is

$$\vec{n} = \frac{\nabla G}{|\nabla G|} \sim \vec{i} - g_{\tilde{y}}\vec{j} - g_{\tilde{z}}\vec{k}$$

and

$$[\vec{Q} \cdot \vec{n}] = 0 \tag{2.30}$$

becomes

$$\left[Ku + \frac{\gamma+1}{2}u^2\right] + [v]g_{\tilde{y}} + [w]g_{\tilde{z}} = 0 \tag{2.31}$$

12

ELEMENT OF
SHOCK SURFACE

STATE$^{(1)}$

STATE$^{(2)}$

$\vec{n}$

$\tilde{y}$

G

x

$\tilde{z}$
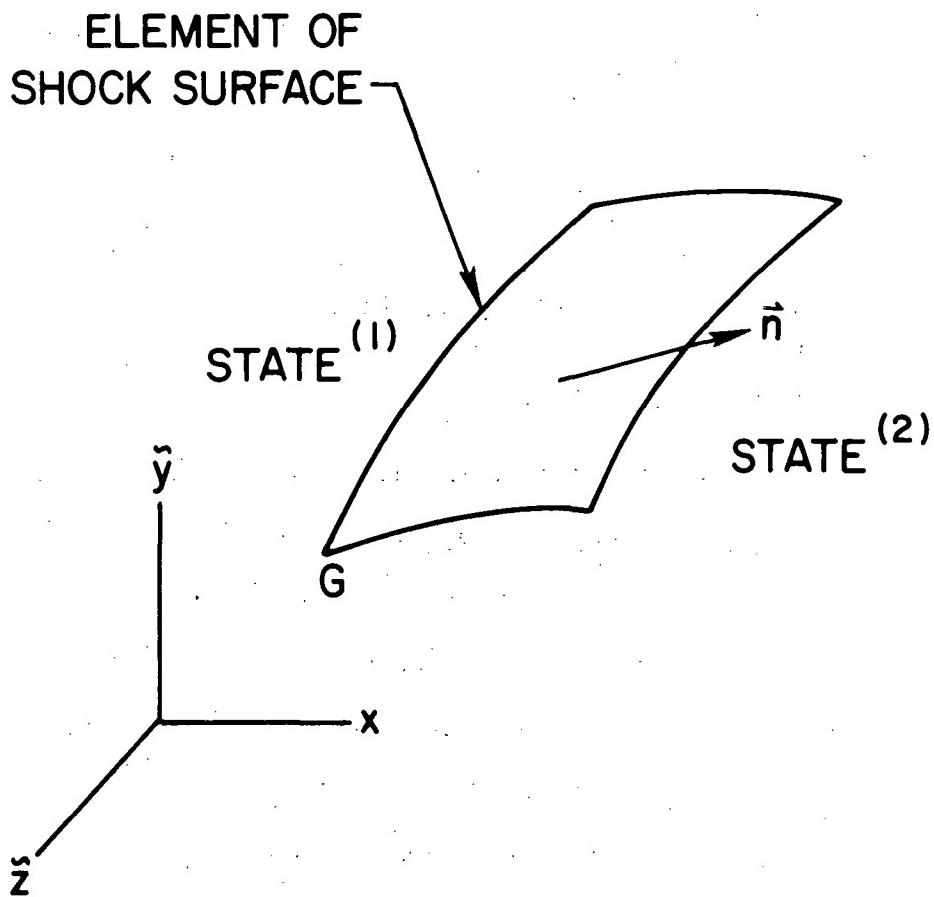
Figure 2.2. Shock Wave Element.

13

where

$$[\ ] = \text{jump} = (\ )^{(2)} - (\ )^{(1)}$$

Since the tangential component of velocity does not jump across the shock

$$[\vec{q} \times \vec{n}] = 0 \tag{2.32}$$

or

$$- [v]g_{\tilde{z}} + [w]g_{\tilde{y}} = 0 \tag{2.33}$$

$$[u]g_{\tilde{z}} + [w] = 0 \tag{2.34}$$

$$[u]g_{\tilde{y}} + [v] = 0 \tag{2.35}$$

Substituting equations (2.33) – (2.35) in equation (2.31) gives

$$- \left[Ku + \frac{\gamma+1}{2} u^2 \right] [u] + [v]^2 + [w]^2 = 0 \tag{2.36}$$

Equation (2.32) implies that the potential may only jump by a constant across the shock. For convenience we shall assume that $[\varphi] = 0$. Note that u, v, w are the perturbation velocity components and are all zero upstream of the shock. On the shock surface the value of the perturbation potential is taken to be zero.

2.3 FORMULATION OF THE BOUNDARY VALUE PROBLEM IN CONICAL COORDINATES

The flow field to be analyzed here is conical, that is, flow properties are constant along radial lines extending from the origin. For this type of a flow the equations derived in the previous section assume special forms. Since the potential is constant along rays it will be a function of the coordinates $\frac{\tilde{z}}{x}$ and $\frac{\tilde{y}}{x}$. Thus we can define conical variables

$$Z = \frac{\tilde{z}}{Bx} = \frac{z}{bx}$$

$$Y = \frac{\tilde{y}}{Bx} = \frac{z}{bx}$$

where $\quad B = b\delta^{1/3}$

In terms of the above conical variables the perturbation potential assumes the form

$$\varphi(x, \tilde{y}, \tilde{z}) = x\, \phi(Z, Y) \tag{2.37}$$

and the transonic equation (2.25) becomes

$$\left\{K + (\gamma+1)\ (\phi - Z\phi_Z - Y\phi_Y)\right\}\ \left\{Z^2\phi_{ZZ} + 2ZY\phi_{YZ} + Y^2\phi_{YY}\right\} = \frac{1}{B^2}\ (\phi_{ZZ} + \phi_{YY}) \tag{2.38}$$

Since the wing is also conical

$$f(x, \frac{\tilde{z}}{b}) = xF(Z)$$

and this makes the boundary condition on the body

$$\phi_Y(Z,0) = B\{F(Z) - ZF'(Z)\} \tag{2.39}$$

The two boundary conditions on the shock then are

$$-\left\{K(Z\phi_Z + Y\phi_Y)^2 - \frac{\gamma+1}{2}\ (Z\phi_Z + Y\phi_Y)^3\right\} + \frac{1}{B^2}\ (\phi_Z^2 + \phi_Y^2) = 0 \tag{2.40}$$

$$\phi = 0 \tag{2.41}$$

It proves useful to write the equation for the perturbation potential in a curvilinear coordinate system. The elliptic cylinder coordinates, which were chosen, have the advantage of fitting well into the numerical scheme.

15

The elliptic cylinder coordinates are given by

$$Z = \cosh \xi \cos \eta$$

$$Y = \sinh \xi \sin \eta$$

for $\xi \geq 0$ and $0 \leq \eta < 2\pi$

Since the wings to be considered are symmetric with respect to the y and z axes, the range of η is $0 \leq \eta \leq \frac{\pi}{2}$ as shown in Figure 2.3. The wing extends from zero to one on the Z axis ($\xi = 0$) and the shock is a curve in the plane; whose shape and location are part of the solution for the potential function.

In the new coordinates the equations for the velocity potential and the boundary condition on the wing become

$$\left\{ K + (\gamma+1) \left(\phi - \frac{1}{J} (\sinh \xi \cosh \xi \, \phi_\xi - \sin \eta \cos \eta \, \phi_\eta) \right) \right\}$$

$$\left\{ \frac{1}{J} \left(\sinh^2 \xi \cosh^2 \xi \, \phi_{\xi\xi} - 2 \sinh \xi \cosh \xi \sin \eta \cos \eta \, \phi_{\xi\eta} + \sin^2 \eta \cos^2 \eta \phi_{\eta\eta} \right) - \right.$$

$$\sinh \xi \cosh \xi \left(\frac{2}{J^2} (\sinh^2 \xi \cosh^2 \xi - \sin^2 \eta \cos^2 \eta) + \right.$$

$$\left. 1 - \frac{1}{J} (\sinh^2 \xi + \cosh^2 \xi) \right) \phi_\xi +$$

$$\sin \eta \cos \eta \left(\frac{2}{J^2} (\sinh^2 \xi \cosh^2 \xi - \sin^2 \eta \cos^2 \eta) + \right.$$

$$\left. 1 + \frac{1}{J} (\cos^2 \eta - \sin^2 \eta) \right) \phi_\eta \bigg\} = \frac{1}{B^2} (\phi_{\xi\xi} + \phi_{\eta\eta}) \qquad (2.42)$$

where

$$J = \sinh^2 \xi + \sin^2 \eta$$

and

$$\phi_\xi(0,\eta) = \phi_Y(\cos \eta, \, 0) \sin \eta \qquad (2.43)$$

16
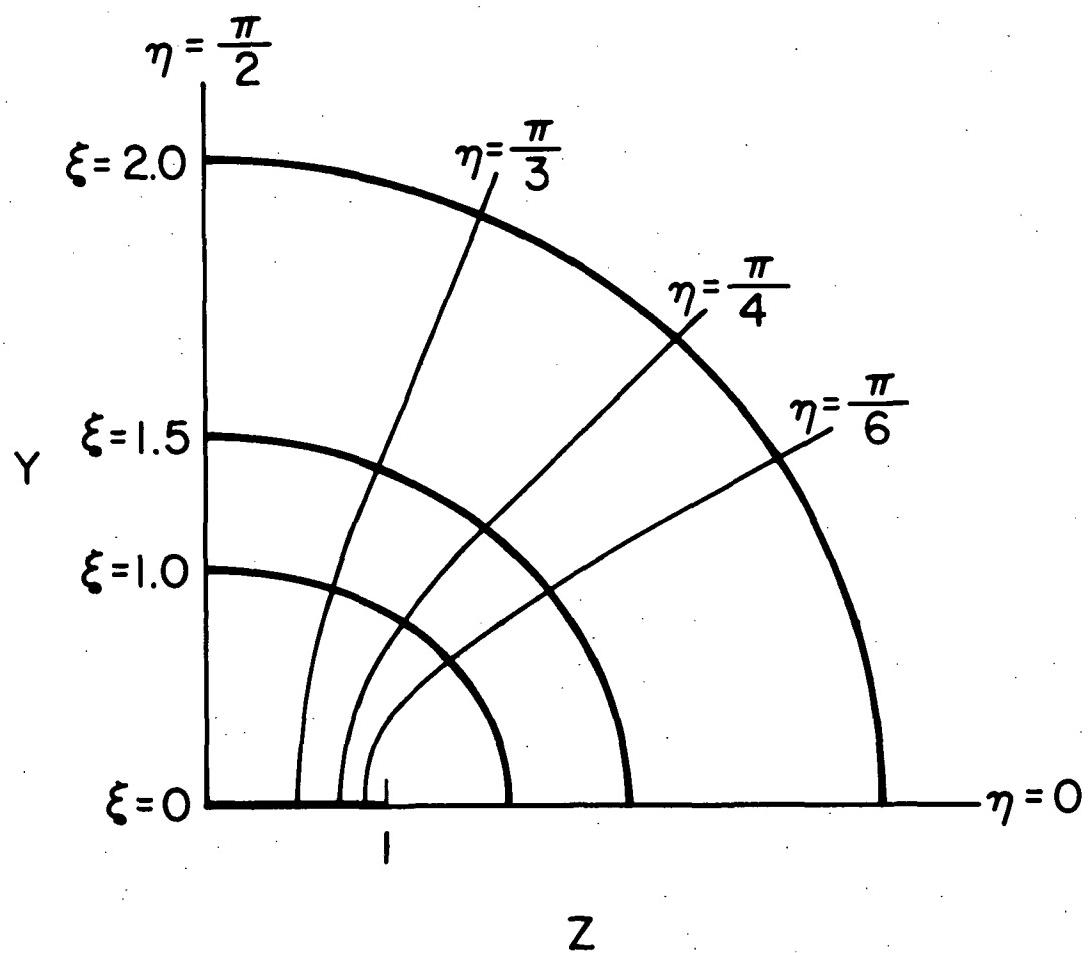
Figure 2.3. Elliptic Cylinder Coordinates.

17

On the shock surface the boundary conditions take the form

$$-\left\{(\sinh\xi\,\cosh\xi\phi_\xi - \sin\eta\,\cos\eta\phi_\eta)^2 - \frac{\gamma+1}{2KJ}(\sinh\xi\,\cosh\xi\phi_\xi - \sin\eta\,\cos\eta\phi_\eta)^3\right\}$$

$$+\frac{1}{B^2K}\left(\phi_\xi^2 + \phi_\eta^2\right)\left(\sinh^2\xi\,\cos^2\eta + \cosh^2\xi\,\sin^2\eta\right) = 0 \tag{2.44}$$

and $\quad \phi = 0 \quad$ on the shock $\tag{2.45}$

Since the potential and the shock are symmetric with respect to the Z and Y axis

$$\phi_\eta = 0 \quad \text{at} \quad \eta = 0, \frac{\pi}{2} \tag{2.46}$$

$$\frac{d\xi}{d\eta} = 0 \quad \text{at} \quad \eta = 0, \frac{\pi}{2} \tag{2.47}$$

Fig. 2.4 gives a summary of the boundary value problem in the cross plane.

Various physical quantities can be derived from the solution of the transonic potential equation. Two which shall be considered here are the pressure coefficient C_p and the drag coefficient C_D.

The pressure coefficient is defined by

$$C_p = \frac{p - p_\infty}{\frac{1}{2}\rho_\infty U^2} = \frac{2}{\gamma M_\infty^2}\left(\frac{p}{p_\infty} - 1\right) \tag{2.48}$$

but

$$\frac{p}{p_\infty} = \left(\frac{a^2}{a_\infty^2}\right)^{\frac{\gamma}{\gamma-1}}$$

and using equations (2.16) and (2.21) we obtain

$$C_p = \frac{2}{\gamma M_\infty^2}\left\{\left(1 - (\gamma-1)M_\infty^2\,\delta^{2/3}\,\varphi_x\right)^{\frac{\gamma}{\gamma-1}} - 1\right\}$$
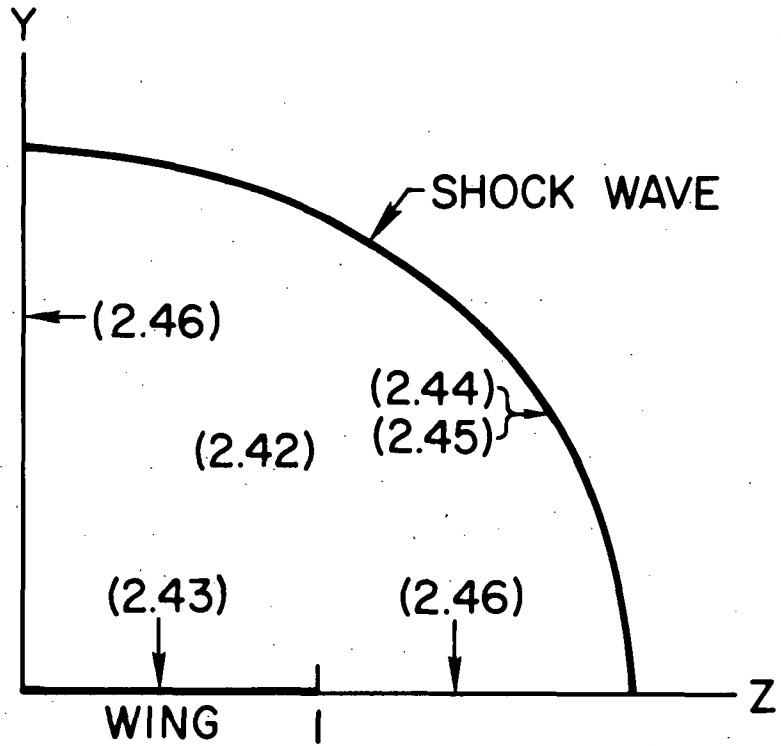
Figure 2.4. Boundary Value Problem for the Cross Plane.

For small perturbations this expression may be expanded in series the result to lowest order being

$$C_p = -2\delta^{2/3}\, \varphi_x$$

In conical coordinates the pressure coefficient on the wing at $x = 1$ takes the form

$$C_p = -2\delta^{2/3}\,(\phi - Z\phi_Z) \qquad\qquad (2.49)$$

The drag coefficient is obtained by integrating the pressure coefficient over the surface of the wing and normalizing to the area of the wing plan form.

$$C_D = \frac{\iint C_p \; dA \; \vec{n} \cdot \vec{i}}{b} \qquad\qquad (2.50)$$

dA is an area element on the wing surface and $\vec{n}$ is the unit vector normal to the wing surface. In conical coordinates equation (2.50) becomes

$$C_D = \delta \int_0^1 C_p(F - ZF')\, dZ \qquad\qquad (2.51)$$

20

CHAPTER 3

NUMERICAL PROCEDURES AND RESULTS

3.1 INTRODUCTORY REMARKS

The transonic equation for the perturbation potential (equation 2.42) has the general form

$$a_1 \phi_{\xi\xi} + 2a_2 \phi_{\xi\eta} + a_3 \phi_{\eta\eta} + a_4 = 0 \qquad (3.1)$$

where the coefficients a_1 through a_4 are function of ξ, η, ϕ_ξ, ϕ_η and the similarity parameters K and B. Depending on the sign of the quantity

$$D = a_2^2 - a_1 a_3$$

equation (3.1) is elliptic parabolic or hyperbolic if D is negative, zero or positive respectively.

For the cases to be considered here, equation (2.42) is of elliptic type within the region bounded by the shock wave (Fig. 2.4) and centered differences are proper to approximate its derivatives.

The shock shape and location are not known a priori. They are part of the solution of equation (2.42). With this in mind a method has been developed that solves simultaneously for the shock shape and location, and the flow potential in an iterative manner. This is done by initially locating the shock near the Mach cone and then proceeding as follows:

(i) Solve equation (2.42) subject to the boundary conditions on the Y and Z axes and $\phi = 0$ on the shock.

(ii) Split equation (2.44) in such a way that a new shock location is obtained using information from step (i)

(iii) Go back to step (i) with the shock at the new location and repeat

the sequence, until the shock location converges.

Equation (2.44) is split in a way that makes the sequence just presented a convergent one.

The following sections give the details of the procedure just described.

3.2 PRESENTATION OF DIFFERENCE FORMULAS AND RELAXATION ALGORITHM

Consider the numerical solution of equation (2.42) with the shock near the Mach cone. The location of the Mach cone is known from linearized theory; at $x = 1$ it is given by

$$R_{MC} = \frac{1}{B\sqrt{K}} = \frac{1}{b\sqrt{M_\infty^2 - 1}}$$

where

$$R_{MC} = \sqrt{Y^2 + Z^2}$$

On the Z axis

$$R_{MC} = Z = \cosh\xi_{MC}$$

and the initial shock location is taken to be

$$\xi_{MC} = \cosh^{-1}\frac{1}{B\sqrt{K}}$$

Two types of boundary conditions occur. On the shock the potential is specified and this is incorporated directly into the difference formulas by taking $\phi_{imax,j} = 0$ for all j. On the other boundaries derivatives are specified and these are incorporated on mesh points which are offset one half mesh spacing from the actual boundary.

22

This gives a simpler and more accurate treatment of the boundary condition.[7]

The grid geometry is rectangular as shown in Figure 3.1 and the difference equations used for the interior points ($i \neq 1$, $j \neq 1$, jmax) are

$$\phi_{\xi i,j} = \frac{\phi_{i+1,j} - \phi_{i-1,j}}{2\Delta\xi} + 0(\Delta\xi^2) \qquad (3.2)$$

$$\phi_{\eta i,j} = \frac{\phi_{i,j+1} - \phi_{i,j-1}}{2\Delta\eta} + 0(\Delta\eta^2) \qquad (3.3)$$

$$\phi_{\xi\xi i,j} = \frac{\phi_{i+1,j} - 2\phi_{i,j} + \phi_{i-1,j}}{\Delta\xi^2} + 0(\Delta\xi^2) \qquad (3.4)$$

$$\phi_{\eta\eta i,j} = \frac{\phi_{i,j+1} - 2\phi_{i,j} + \phi_{i,j-1}}{\Delta\eta^2} + 0(\Delta\eta^2) \qquad (3.5)$$

$$\phi_{\xi\eta i,j} = \frac{\phi_{i+1,j+1} - \phi_{i+1,j-1} - \phi_{i-1,j+1} + \phi_{i-1,j-1}}{4\Delta\xi\Delta\eta} + 0(\Delta\xi\Delta\eta) \quad (3.6)$$

where the subscripts i,j give the location where the solution is computed. These difference equations are second order accurate.

For grid points along $i = 1$, $j = 1$, or $j = $ jmax the difference formulas are modified to incorporate the specified values of ϕ_ξ and ϕ_η which are given along $\xi = 0$ and $\eta = 0$, $\frac{\pi}{2}$, respectively. To illustrate this consider a grid point at $i = 1$ for all j. This point is a distance $\frac{\Delta\xi}{2}$ away from the boundary $\xi = 0$ where ϕ_ξ is known from equation (2.43), and is denoted by $PC(\xi)$.
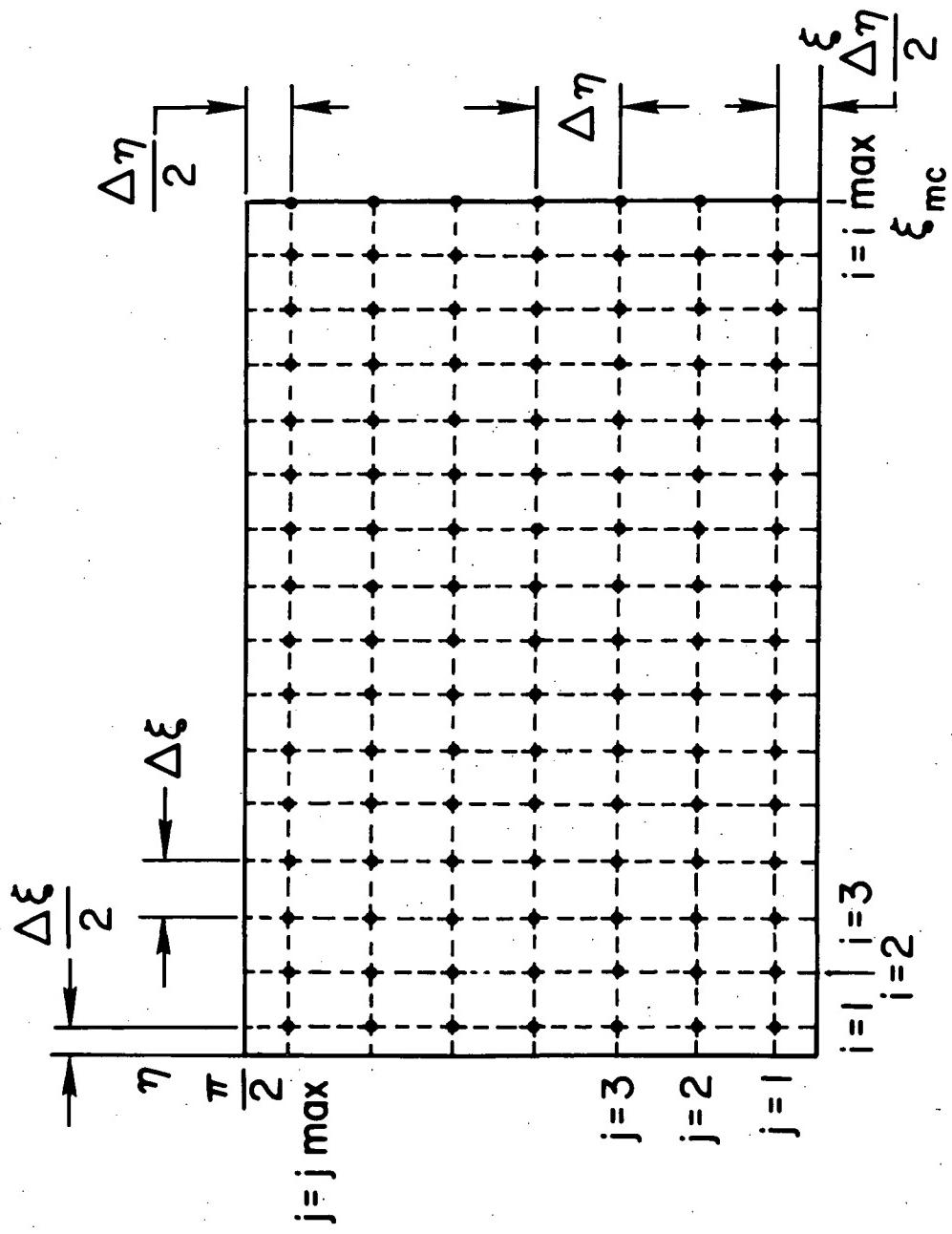
Figure 3.1. Grid Geometry for the Shock Wave at ζ_{mc}.

With a fictitious mesh point at $i = -1$
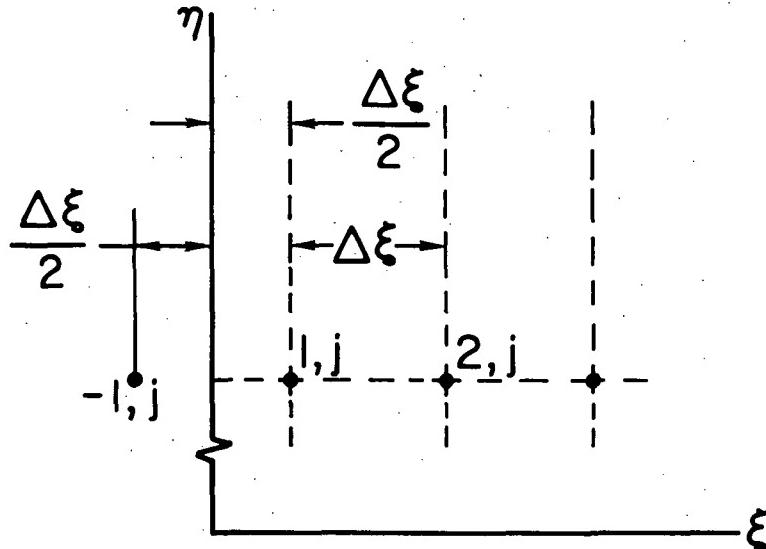
ϕ_ξ at $i = 1$ can be written as

$$\phi_{\xi 1,j} = \frac{\phi_{2,j} - \phi_{-1,j}}{2\Delta\xi} = \frac{\phi_{2,j} - \phi_{1,j} + \phi_{1,j} - \phi_{-1,j}}{2\Delta\xi} =$$

$$= \frac{\phi_{2,j} - \phi_{1,j}}{2\Delta\xi} + \frac{1}{2}\frac{\phi_{1,j} - \phi_{-1,j}}{\Delta\xi}$$

giving $\phi_{\xi 1,j} = \dfrac{\phi_{2,j} - \phi_{1,j}}{2\Delta\xi} + \dfrac{1}{2} PC(j)$ \hfill (3.7)

$\phi_{\xi\xi}$ is evaluated in a similar fashion, giving

$$\phi_{\xi\xi 1,j} = \frac{\dfrac{\phi_{2,j} - \phi_{1,j}}{\Delta\xi} - PC(j)}{\Delta\xi} = \frac{\phi_{2,j} - \phi_{1,j}}{\Delta\xi^2} - \frac{1}{\Delta\xi} PC(j) \qquad (3.8)$$

For the mixed derivative $\phi_{\xi\eta}$ at $i = 1$ three different forms appear depending on the value of j. If $j \neq 1$ or $jmax$ we can make the approximation

$$\phi_{\xi\eta 1,j} = \frac{\phi_{\xi 1,j+1} - \phi_{\xi 1,j-1}}{2\Delta\eta}$$

and use equation (3.7) to obtain

$$\phi_{\xi\eta 1,j} = \frac{1}{4\Delta\eta}\left(PC(j+1)-PC(j-1) + \frac{\phi_{2,j+1}-\phi_{1,j+1}-\phi_{2,j-1}+\phi_{1,j-1}}{\Delta\xi}\right) \quad (3.9)$$

If $i = 1$ and $j = 1$ (or jmax), $\phi_{\xi\eta}$ is computed by averaging the values
of $\phi_{\xi\eta}$ at neighboring points as shown below.
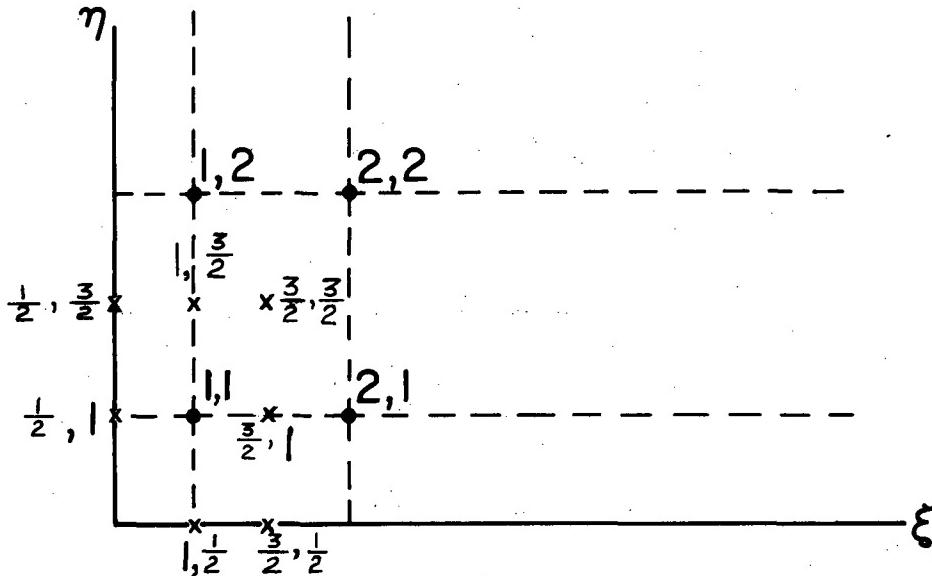
$$\phi_{\xi\eta 1,1} = \frac{1}{4}\left(\phi_{\xi\eta 1,\frac{1}{2}} + \phi_{\xi\eta\frac{1}{2},1} + \phi_{\xi\eta 1,\frac{3}{2}} + \phi_{\xi\eta\frac{3}{2},1}\right)$$

but

$$\phi_{\xi\eta 1,\frac{1}{2}} = 0 \quad \text{since} \quad \phi_{\eta} = 0 \quad \text{on} \quad \eta = 0$$

and $\phi_{\xi\eta}$ on $\xi = 0$ can be calculated from equation (2.43) and will be
denoted by PCA(j) giving

$$\phi_{\xi\eta 1,1} = \frac{1}{4}\left(PCA(1) + \frac{1}{2}PCA(\frac{3}{2}) + \frac{\phi_{1,1}-\phi_{2,1}-\phi_{1,2}+\phi_{2,2}}{4\Delta\xi\Delta\eta}\right) \quad (3.10)$$

Similarly special forms for ϕ_η and $\phi_{\eta\eta}$, on $j = 1$ and $j = $ jmax for all i, and $\phi_{\xi\eta}$ for $i = 1$, $j = $ jmax are derived with the result summarized in Table 3.1.

The difference equations just presented are used in equation (3.1) and a difference equation for $\phi_{i,j}$ is obtained. This equation is linearized, by evaluating the coefficients a_1, a_2 and a_3 using values of $\phi_{i,j}$ from the previous iteration, and solved by a point relaxation algorithm whose formula is

$$\phi_{i,j}^{(n+1)} = \omega \hat{\phi}_{i,j}^{(n+1)} + (1 - \omega)\phi_{i,j}^{(n)} \tag{3.11}$$

where $\phi_{i,j}^{(n)}$ is the value at the nth iteration

$\quad\quad \hat{\phi}_{i,j}^{(n+1)} \quad\quad\quad " \quad\quad\quad (n+1)$th $\quad "$

$\quad\quad \phi_{i,j}^{(n+1)}$ is the relaxed value

$\quad\quad \omega \quad\quad$ is the relaxation parameter

3.3 MOVING THE SHOCK

On the shock $\phi = 0$ and we can write

$$\phi_\xi \, d\xi + \phi_\eta \, d\eta = 0$$

or

$$\frac{d\xi}{d\eta} = -\frac{\phi_\eta}{\phi_\xi} \quad\quad \text{on the shock}$$

and upon substituting the above in equation (2.44) and rearranging it we obtain the relation

27

Table 3.1

Difference Equations for the Transonic Potential Equation

	i ≠ 1	i = 1
j ≠ 1,jmax	(3.2) (3.3) (3.4) (3.5) (3.6)	(3.7) (3.3) (3.8) (3.5) (3.9)
j = 1	$\phi_{\eta 1,1} = \dfrac{\phi_{1,2} - \phi_{1,1}}{2\Delta\eta}$ (3.2) $\phi_{\eta\eta 1,1} = \dfrac{\phi_{1,2} - \phi_{1,1}}{\Delta\eta^2}$ (3.4) $\phi_{\xi\eta 1,1} = \dfrac{1}{4\Delta\xi\Delta\eta}\left(\phi_{i+1,2} - \phi_{i+1,1} - \phi_{i-1,2} + \phi_{i-1,1}\right)$	$\phi_{\eta 1,1} = \dfrac{\phi_{1,2} - \phi_{1,1}}{2\Delta\eta}$ (3.7) $\phi_{\eta\eta 1,1} = \dfrac{\phi_{1,2} - \phi_{1,1}}{\Delta\eta^2}$ (3.8) (3.10)
j = jmax	$\phi_{\eta 1,jmax} = \dfrac{\phi_{1,jmax} - \phi_{1,jmax-1}}{2\Delta\eta}$ (3.2) $\phi_{\eta\eta 1,jmax} = \dfrac{\phi_{1,jmax-1} - \phi_{1,jmax}}{\Delta\eta^2}$ (3.4) $\phi_{\xi\eta 1,jmax} = \dfrac{1}{\Delta\xi\Delta\eta}\left(\phi_{i+1,jmax} - \phi_{i+1,jmax-1} - \phi_{i-1,jmax} + \phi_{i-1,jmax-1}\right)$	$\phi_{\eta 1,jmax} = \dfrac{\phi_{1,jmax} - \phi_{1,jmax-1}}{2\Delta\eta}$ (3.7) $\phi_{\eta\eta 1,jmax} = \dfrac{\phi_{1,jmax-1} - \phi_{1,jmax}}{\Delta\eta^2}$ (3.8) $\phi_{\xi\eta 1,jmax} = \dfrac{1}{4}\left[\text{PCA}\left(jmax - \tfrac{1}{2}\right) + \tfrac{1}{2}\text{PCA}\left(jmax-1\right) - \dfrac{1}{4\Delta\xi\Delta\eta}\right]$ $\left(\phi_{1,jmax} - \phi_{2,jmax} - \phi_{1,jmax-1} + \phi_{2,jmax-1}\right)$

$$\sinh^2\xi \, \cosh^2\xi = -\left\{ 2\left(\frac{d\xi}{d\eta}\right)\sinh\xi \, \cosh\xi \, \sin\eta \, \cos\eta + \sin^2\eta \, \cos^2\eta \left(\frac{d\xi}{d\eta}\right)^2 - \right.$$

$$\frac{\gamma+1}{2JK} \, \phi_\xi \left[\sinh\xi \, \cosh\xi + \sin\eta \, \cos\eta\left(\frac{d\xi}{d\eta}\right)\right]^3 \Bigg\}$$

$$\left. + \frac{1}{B^2K}\left[1 + \left(\frac{d\xi}{d\eta}\right)^2\right]\left(\sinh^2\xi \, \cos^2\eta + \cosh^2\xi \, \sin^2\eta\right)\right\} \qquad (3.12)$$

With the solution just obtained the right hand side of equation (3.12) is computed and a corrected new shock location is obtained whose shape is usually non elliptic. Since the same number of mesh points are kept, so that the shock is always on grid points, the new grid geometry is non-rectangular and $\Delta\xi$ is now a function of η. A subscript j will be used, $\Delta\xi_j$, to show this dependence. Note that grid points which have the same value for the subscript i are not aligned on vertical lines any more.

The values for the potential (with the shock at ξ_{MC}) are transferred to the new grid points and are used as starting values for the relaxation procedure.

In calculating η derivatives (at a given i) values of ϕ on a vertical line are needed, thus requiring interpolated values of ϕ at points where the solution is not computed. Figure 3.2 shows these points (marked by x's) when the derivative is calculated at i,j. The values of the potential at these points are calculated applying a second order accurate interpolation formula which uses values of the potential at the three nearest grid points. For example the value of ϕ at a point s away from i, j+1 is
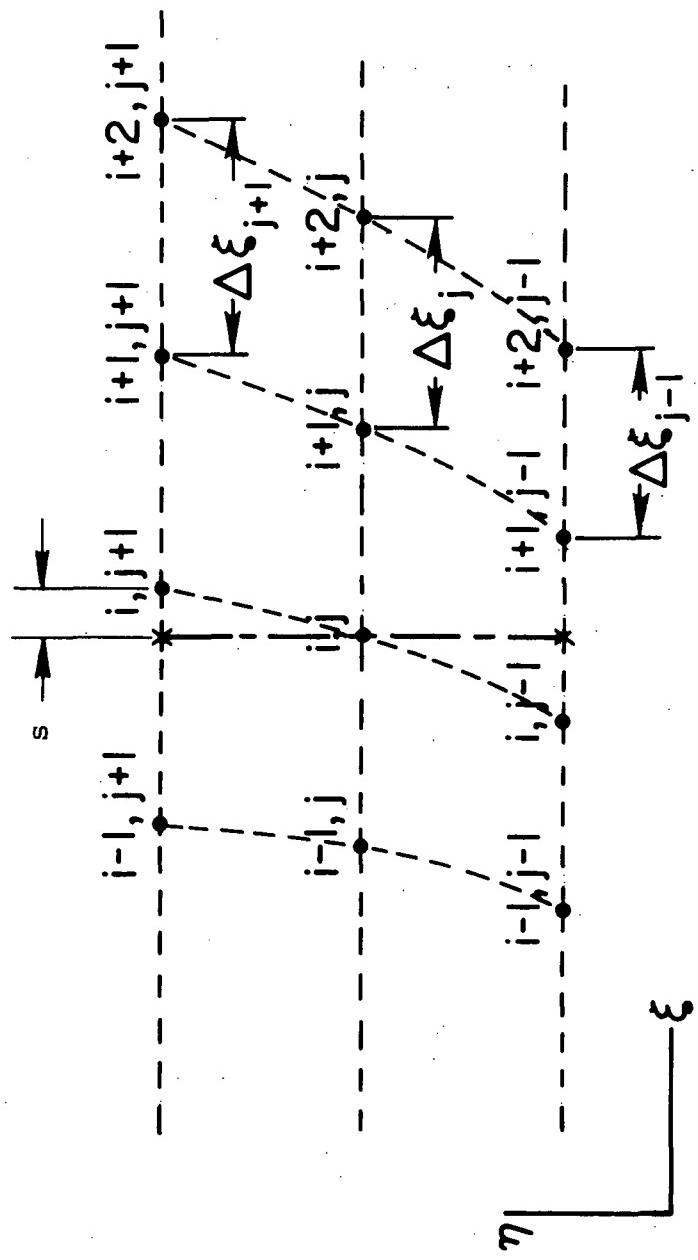
Figure 3.2. Variable Grid Geometry.

30

$$\phi_{s,j+1} = \phi_{i,j+1} + s\left(\phi_{i,j+1} - \phi_{i-1,j+1}\right) + \frac{s(s+1)}{2}\left(\phi_{i+1,j+1} - 2\phi_{i,j+1} + \phi_{i-1,j+1}\right)$$

This interpolation formula has the same accuracy as the difference equations. The solution for ϕ is analytical in the neighborhood of the point i,j+1, therefore the overall accuracy of the numerical scheme is preserved.

3.4 COMPUTATIONAL DETAILS

Sections 3.2 and 3.3 give the basic method for solving the transonic potential equation. In applying these principles certain points must be resolved. These include choice of relaxation parameter, number of grid points used as well as the determination of convergence of the iterative scheme and overall accuracy.

The choice of the relaxation parameter (ω) determines the rate of convergence of the algorithm. For Laplace's equation an optimal value can be found from the spectral radius of the Gauss-Seidell method.[11] The transonic equation is nonlinear and such a value must be found by experiment since it does not have an explicit form. The value of ω that gave the fastest convergence (fewest number of iterations) for a grid with 40x20 points, in the ξ and η respectively, B = .2 and K = 3.0 is 1.93. This value was used for all the computation since ω did not depend strongly on B and K.

The convergence of the solution, for a particular shock location, is based on the value of the residue – the difference in the potential at a given grid point on two successive iterations. When the value of the residue at all points in the field is less than 2.5×10^{-5} the

solution is assumed to have converged. The same criterion is used for the shock location with 10^{-4} as the reference tolerance. Table 3.2 gives the number of iterations needed for convergence (n) and the shock location (value of $\frac{z}{b}$) on $\eta = 0$. The location prescribed initially to the shock wave is 2.65000; the rest are corrected locations obtained from equation (3.12).

Table 3.2

Successive Shock Wave Locations

K = 3.00	B = .2
n	$\frac{z}{b}$
118	2.65000
80	2.79355
66	2.86181
62	2.89161
48	2.90411
21	2.90925
9	2.91132
5.	2.91216
2	2.91249
1	2.91265
	2.91267

The accuracy of the methods has been tested by mesh variation. For shock locations more than one span away from the tip of the wing the grid used has 40 points in the ξ direction and 20 in the η direction. However, for cases with the shock closer to the tip of the wing a 20 x 20 grid is sufficient.

In calculating the pressure coefficient, values of the potential on the wing are needed. These are evaluated by extending the solution to the wing surface using a second order accurate extrapolation equation which has the formula

$$\phi_{\frac{1}{2},j} = \phi_{1,j} - \frac{1}{2}\left(\phi_{2,j} - \phi_{1,j}\right) + \frac{3}{8}\left(\phi_{1,j} - 2\phi_{2,j} + \phi_{3,j}\right)$$

The drag coefficient integral, equation (2.51), is evaluated numerically using the trapezoidal rule.

This section shall conclude with a word about computation times. Two different time scales appear in this problem. Consider starting a computation for one set of conditions (B and K) from the solution to a different problem. If in the new problem the shock location is significantly different a well converged solution may take 15 cycles (shock location corrections.) If solutions are sequenced so that shock locations do not change by much the same degree of convergence may take only 8-10 cycles. A computation that requires 10 cycles, on a grid of 40 x 20, takes about 40 seconds on an IBM 360/91 using double precision arithmetic.

3.5 RESULTS

In this section computed results based on the theory of the previous sections is presented. Two different conical wings, one of rhombic cross section the other circular, are considered for various values of the similarity parameters K and B. The methods can be used to compute other wings which are pointed at the tip.

In conical variables the rhombic wing is given by

$$F(Z) = 1 - Z \qquad 0 \leq Z \leq 1 \qquad (3.13)$$

This equation corresponds to

$$y = \delta x F(Z) = \delta x \left(1 - \frac{z}{bx}\right) \tag{3.14}$$

in the physical coordinates and simplifies to

$$y = \delta \left(1 - \frac{z}{b}\right)$$

at $x = 1$.

For the circular wing

$$F(Z) = 1 - Z^2 \qquad 0 \leq Z \leq 1 \tag{3.15}$$

and in the physical coordinates it becomes

$$y = \delta \left(1 - \frac{z^2}{b^2}\right)$$

at $x = 1$.

Figures 3.3 and 3.4 give the shape and location of the shock wave in in the cross plane. Figures 3.5, 3.6 and 3.7 give the pressure coefficient along the wing surface for the indicated values of K and B.

34
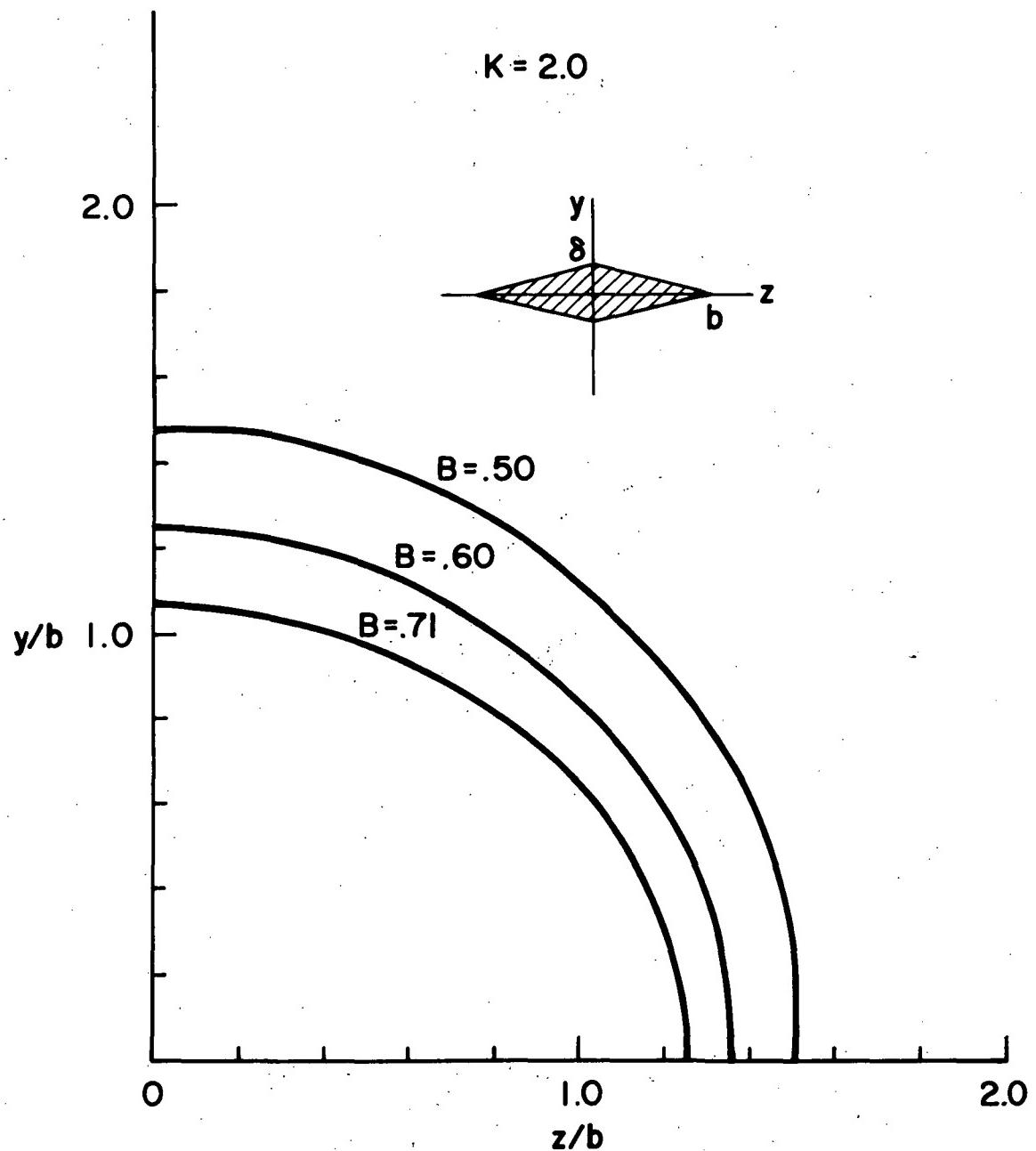
Figure 3.3. Shock Waves for a Rhombic Wing at K = 2.0.

35
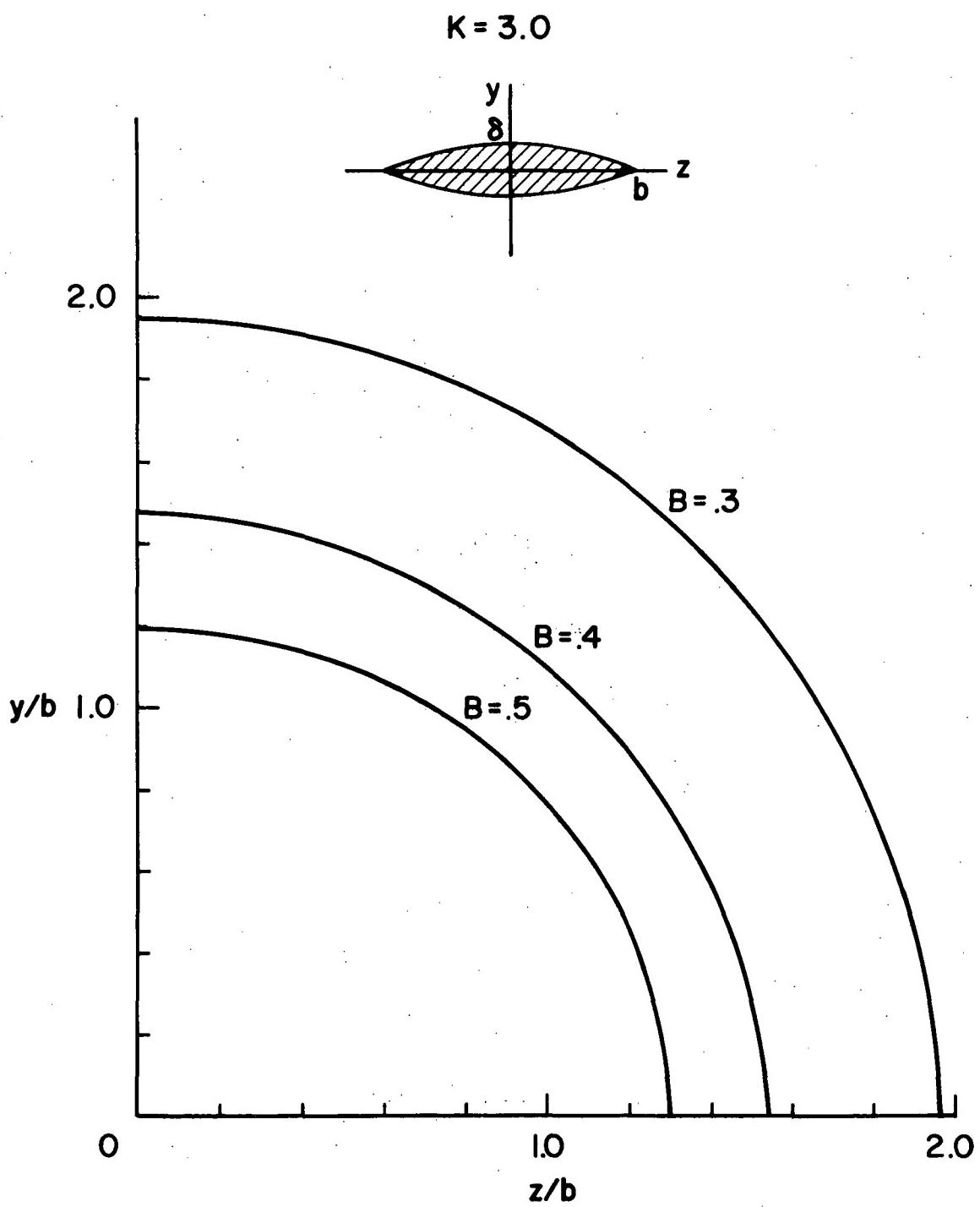
Figure 3.4. Shock Waves for a Circular Wing at K = 3.0.
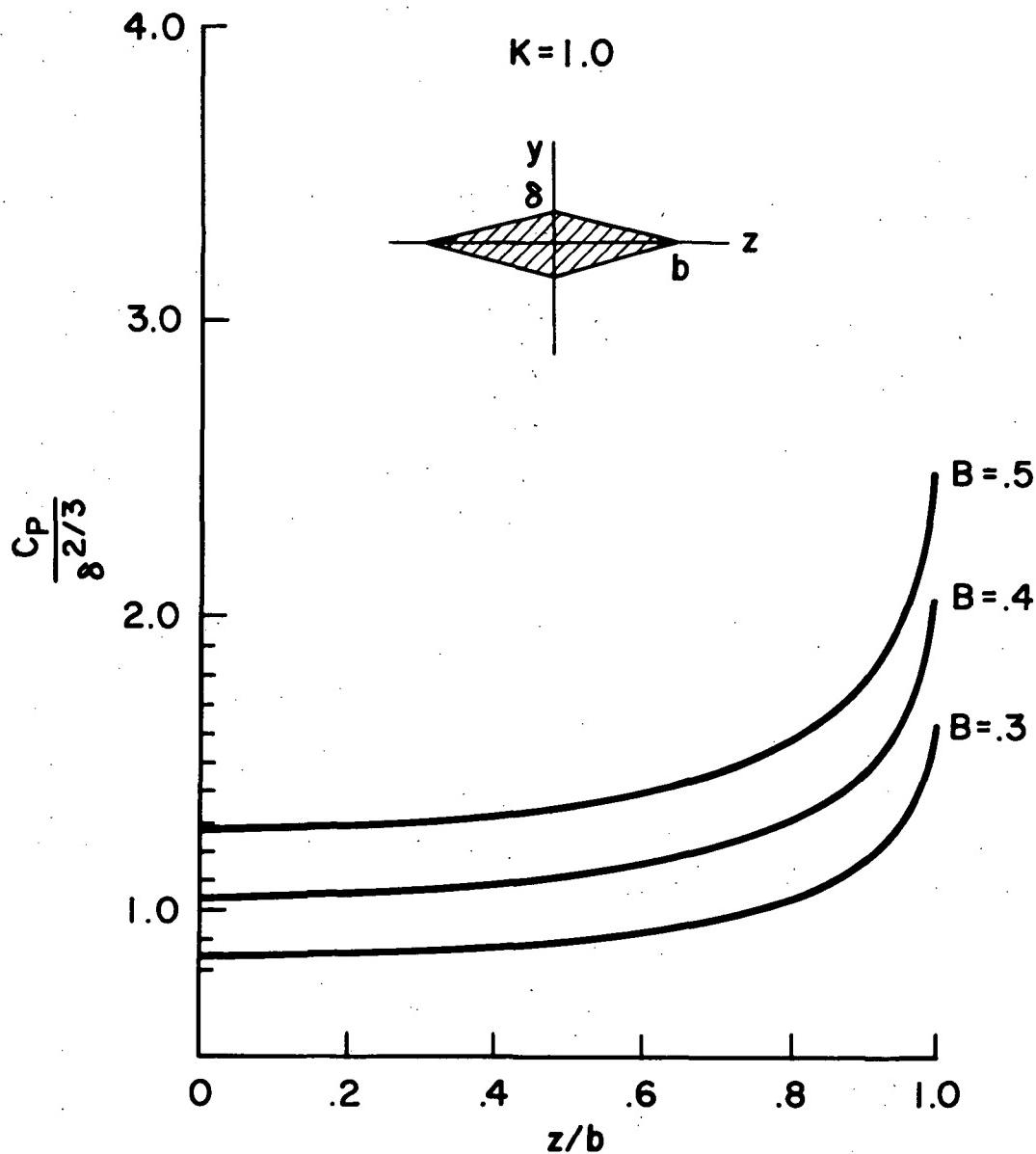
Figure 3.5. Pressure Distributions on the Surface of a Rhombic Wing for K = 1.0.

37
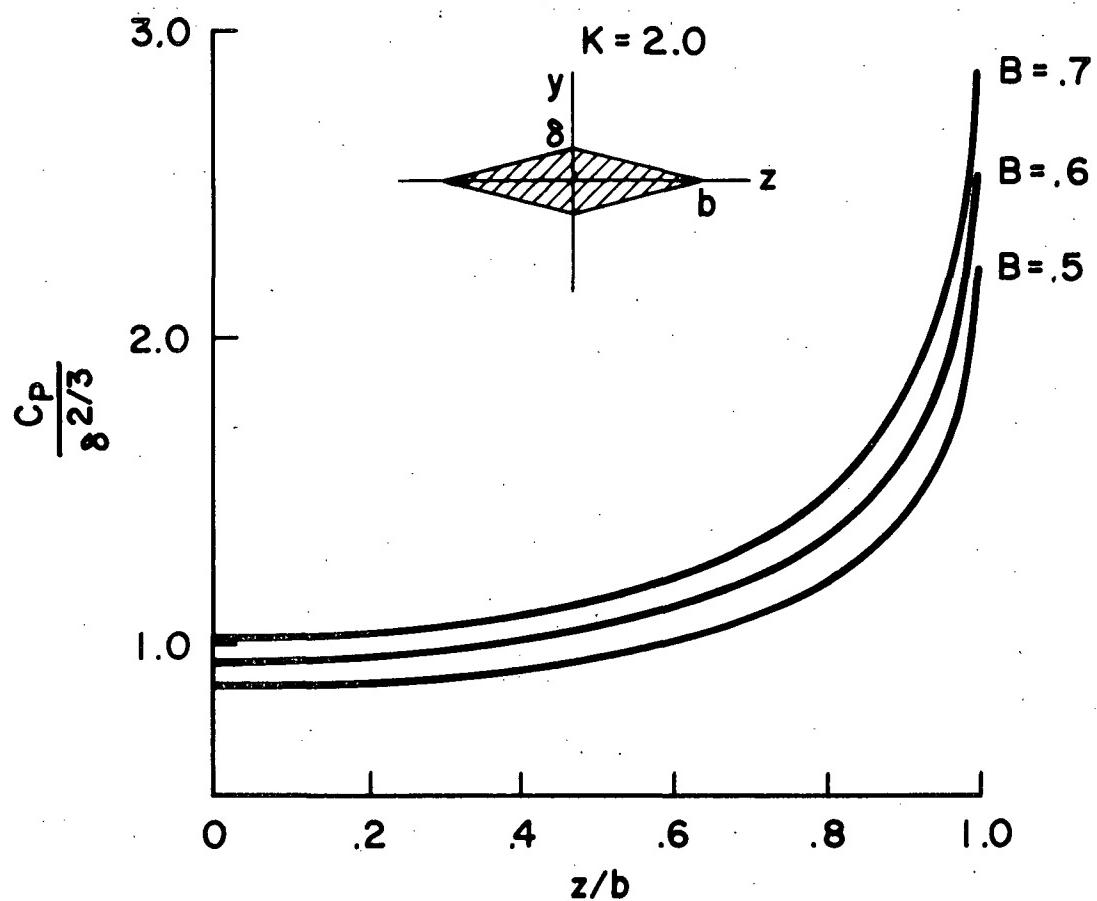
Figure 3.6. Pressure Distributions on the Surface of a Rhombic Wing for K = 2.0.
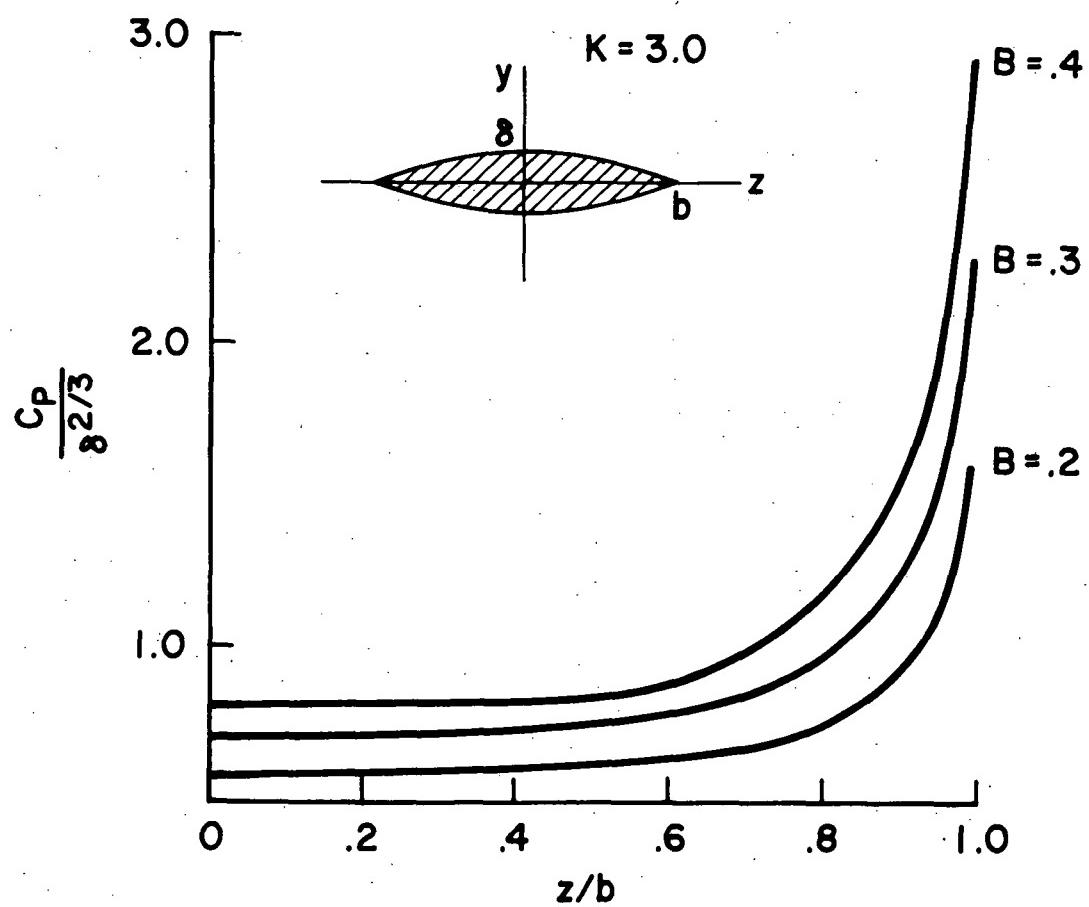
Figure 3.7. Pressure Distributions on the Surface of a Circular Wing for K = 3.0.

39

Page Intentionally Left Blank

CHAPTER 4

SLENDER WINGS

4.1 SLENDER WING THEORY

In this section the theory of "slender" wings will be presented. This theory has been studied by several authors, but the formulation given by Messiter[12] for the non-lifting case is particularly suitable for our purpose. The problem can be defined in several ways, all of which are equivalent. From a mathematical point of view the fundamental assumption is that the solution for the potential near the wing (inner expansion) is essentially different from the solution near the shock wave (outer expansion). Using a physical picture one could take the reduced aspect ratio, $b\sqrt{M_\infty^2 - 1}$, as a basic parameter and discuss the solution as it tends to zero. Another possibility is to start from non-slender wings and require the parameter B to approach zero with δ, subject to the restriction that $\frac{\delta}{b}$ also approaches zero in order that the wing remain thin. The last choice is the most convenient and is used to obtain inner and outer expansions for the potential. The inner expansion corresponds to the solution of the Laplace equation in the cross plane, incompressible flow, and the outer expansion to axisymmetric, non-linear transonic, flow about an equivalent body of revolution.

This equivalent body is defined as the body of circular cross-section which has the same longitudinal distribution of cross-sectional area as the wing. The equivalent body is defined by

$$r = \delta_e \ E(x) \tag{4.1}$$

where

$$r = \sqrt{y^2 + z^2}$$

$E(x)$ is the longitudinal cross-sectional area distribution and δ_e is the equivalent radius at $x = 1$.

The cross-sectional area of the wing, at $x = 1$, expressed in terms of the equivalent radius is related to the wing dimensions by the constant of proportionality k

$$\pi\delta_e^2 = \pi k b \delta = \pi k \delta^{2/3} B \qquad (4.2)$$

For the outer expansion

$$\varphi^*(x, r^*; K_e) = \delta_e^2 \left\{ E(x)E'(x) \log r^* + g_1(x; K_e) \right\} \qquad (4.3)$$

$$r^* = r\delta_e$$

$$K_e = \frac{M_\infty^2 - 1}{\delta_e^2} \qquad \text{(similarity parameter for axisymmetric flow)} \quad (4.4)$$

and for the inner expansion

$$\overline{\varphi}(x, \overline{y}, \overline{z}; K_e) = \delta_e^2 \overline{\varphi}_1 \log (b\delta_e) + \delta_e^2 \overline{\varphi}_2 \qquad (4.5)$$

where

$$\overline{y} = \frac{y}{b}, \quad \overline{z} = \frac{z}{b}$$

$$\overline{\varphi}_1 = E(x)E'(x) \qquad (4.6)$$

$$\overline{\varphi}_2 = \frac{1}{\pi k} \int_{s_1(x)}^{s_1(x)} h_x(x, \overline{\sigma}) \log\sqrt{\overline{y}^2 + (\overline{z} - \overline{\sigma})^2}\, d\overline{\sigma} + g_1(x; Ke) \qquad (4.7)$$

$g_1(x; K_e)$ is the essential unknown part of the pressure distribution and can only be determined from the solution of the outer problem. The

limits of the integral describe the wing plan form and $y = \delta h(x, \frac{z}{b})$ gives the shape of the wing.

The pressure coefficient C_p is obtained from the inner solution and has the formula[12]

$$\frac{C_p}{\delta_e^2} = -2\left(\overline{\varphi}_{1x} \log(b\delta_e) + \overline{\varphi}_{2x}\right) \tag{4.8}$$

4.2 CONICAL SLENDER WINGS

The equations for slender wings presented in the previous section can be simplified using the properties of conical flows. For conical wings.

$$E(x) = x$$

$$h(x, \overline{\sigma}) = xF(\Sigma) \quad , \qquad \Sigma = \frac{\overline{\sigma}}{x}$$

$$h_x(x, \overline{\sigma}) = F(\Sigma) - \Sigma F'(\Sigma)$$

and since the potential is a conical variable

$$g_1(x; K_e) = -x\log x + xC_1(K_c) \tag{4.9}$$

With the above information, equation (4.7) can be written as

$$\overline{\varphi}_2 = \frac{x}{\pi k} \int_{-1}^{1} (F - \Sigma F') \left\{ \log x + \log\sqrt{Y^2 + (Z - \Sigma)^2} \right\} d\Sigma$$

$$- x \log x + xC_1(K_e) \tag{4.10}$$

and since

$$\frac{1}{\pi k} \int_{-1}^{1} (F - \Sigma F') d\Sigma = \frac{4}{\pi k} \int_{0}^{1} F d\Sigma = 1$$

$$\overline{\varphi}_2 = \frac{x}{\pi k} \int_{-1}^{1} (F - \Sigma F') \log |Z - \Sigma| \, d\Sigma + xC_1(K_e) \qquad (4.11)$$

on $Y = 0$.

From equation (4.2) $\qquad \delta_e^2 = kB\delta^{2/3} \qquad$ so

$$K_e = \frac{K}{kB} \qquad (4.12)$$

and

$$b\delta_e = k^{1/2} B^{3/2}$$

The expression for the pressure coefficient at $x = 1$ then becomes

$$\frac{C_P}{\delta_e^2} = - \left\{ \log k + 3 \log B + 2 \overline{\varphi}_{2x} \right\}$$

or in terms of δ

$$\frac{C_P}{\delta^{2/3}} = - kB \left\{ \log k + 3 \log B + 2 \overline{\varphi}_{2x} \right\} \qquad (4.13)$$

For the rhombus $k = \frac{2}{\pi}$ and $F = 1 - Z$ thus giving

$$\frac{C_P}{\delta^{2/3}} = - \frac{2}{\pi} B \left\{ \log \frac{2}{\pi} + 3 \log B + \log(1-Z^2) - 2 + 2C_1(K_e) \right\} \qquad (4.14)$$

The result for the circular arc where $k = \frac{8}{3\pi}$ and $F = 1 - Z^2$ is

$$\frac{C_P}{\delta^{2/3}} = - \frac{8}{3\pi} B \left\{ \log \frac{8}{3\pi} + 3 \log B + Z^2 - \frac{1}{2} Z^3 \log \frac{(1+Z)}{(1-Z)} + \right.$$

$$\left. \frac{3}{2} \log (1-Z^2) - \frac{5}{3} + 2C_1(K_e) \right\} \qquad (4.15)$$

44

The drag coefficient can now be calculated using the above two equations and performing the integration in equation (2.51) gives:

Rhombus

$$\frac{C_D}{\delta^{5/3}} = \frac{2}{\pi} B \left\{ 4 - \left(\log \frac{2}{\pi} + 2 \log 2 + 3 \log B \right) - 2C_1(K_e) \right\} \qquad (4.16)$$

Circular Arc

$$\frac{C_D}{\delta^{5/3}} = \frac{8}{3\pi} B \left\{ \frac{119}{18} - \frac{4}{3} \left(\log \frac{8}{3\pi} + 3 \log 2 + 3 \log B \right) - \frac{8}{3} C_1(K_e) \right\} (4.17)$$

In order to make the formulation for the pressure and drag coefficients complete, we must compute $C_1(K_e)$. This can be done in several ways. One method of obtaining $C_1(K_e)$ is to integrate the first order transonic equation for flow past a slender cone.[14] A second method is to use the value of the pressure coefficient, on the surface of a slender cone from Kopal's table,[13] in the similarity law given by the equation[14]

$$- 2C_1(K_e) = \frac{C_P^+}{\sigma^2} + 4 \log \sigma - 1$$

C_P^+ is the pressure coefficient on the surface of the cone, and σ is the tangent of the cone semi-vertex angle.

Yet another method is to compare the pressure coefficient obtained numerically, for a particular shape, with the slender wing formula for that particular shape and choose $C_1(K_e)$ such that the two have the same value at a given location on the wing. The location that was chosen is at $Z = 0$. This method also serves as a check on slender body theory since the results obtained numerically represent the solution of a higher order equation.

45

In Figure 4.1, $2C_1(K_e)$ computed using Kopal's table is indicated by the solid curve whereas the results obtained by matching are shown by triangles and squares.

4.3 COMPARISON OF RESULTS

The comparison between the results obtained numerically and the slender wing solution, equations (4.14), (4.15), (4.16) and (4.17), is shown in Figures 4.2 - 4.7.
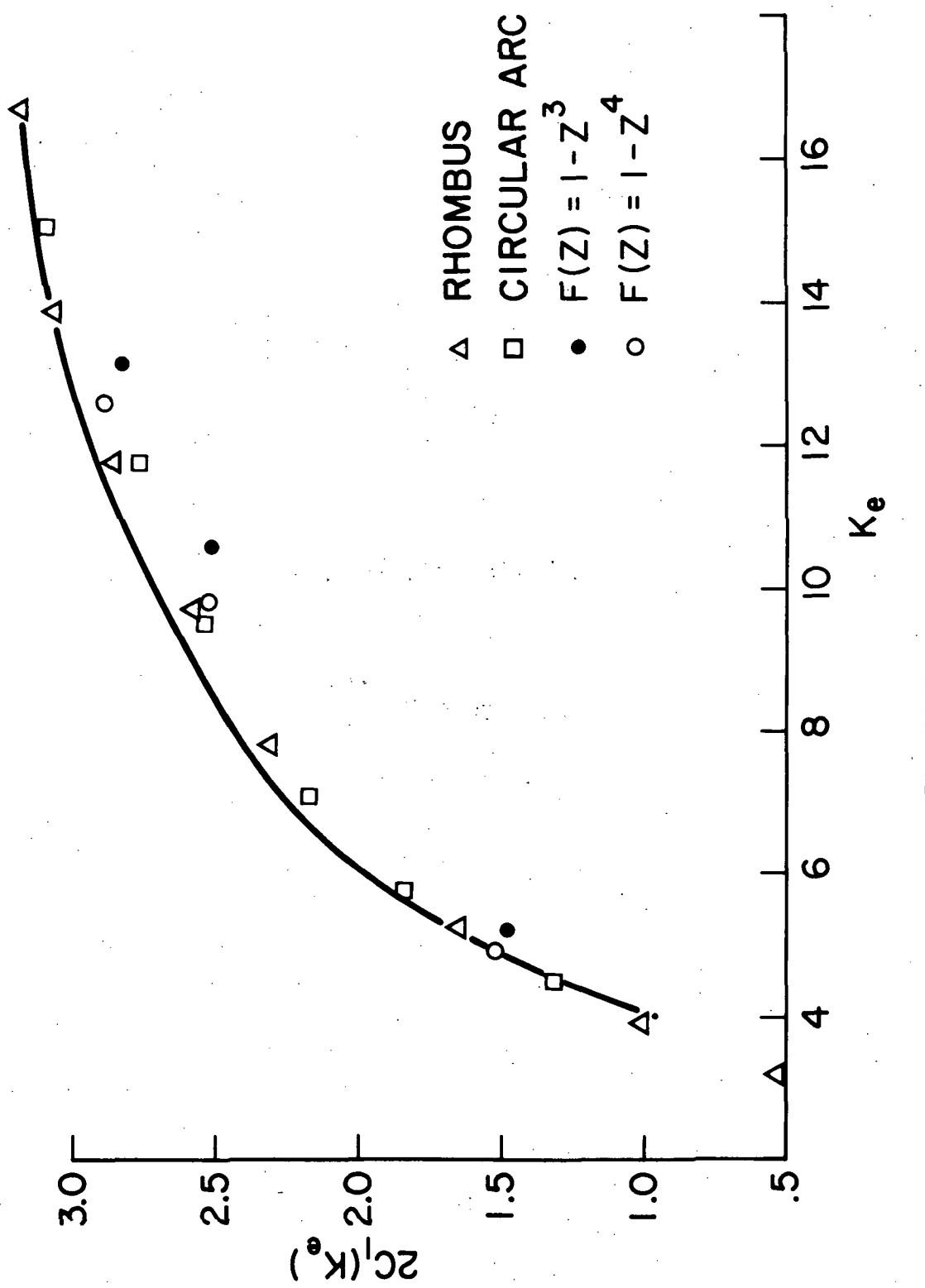
Figure 4.1. The Function $C_1(K_e)$.
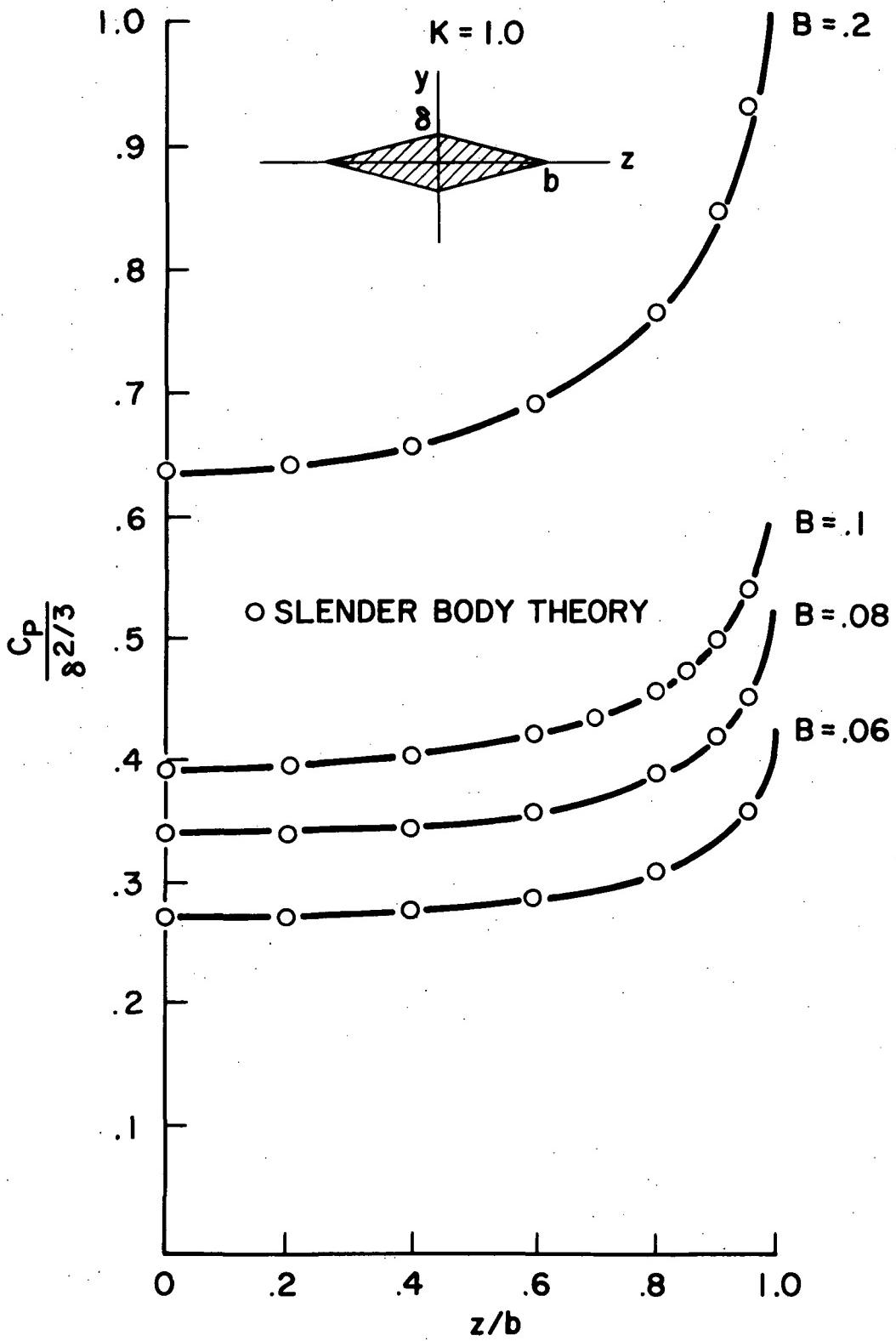
Figure 4.2. Pressure Distributions on the Surface of a Rhombic Wing for K = 1.0.
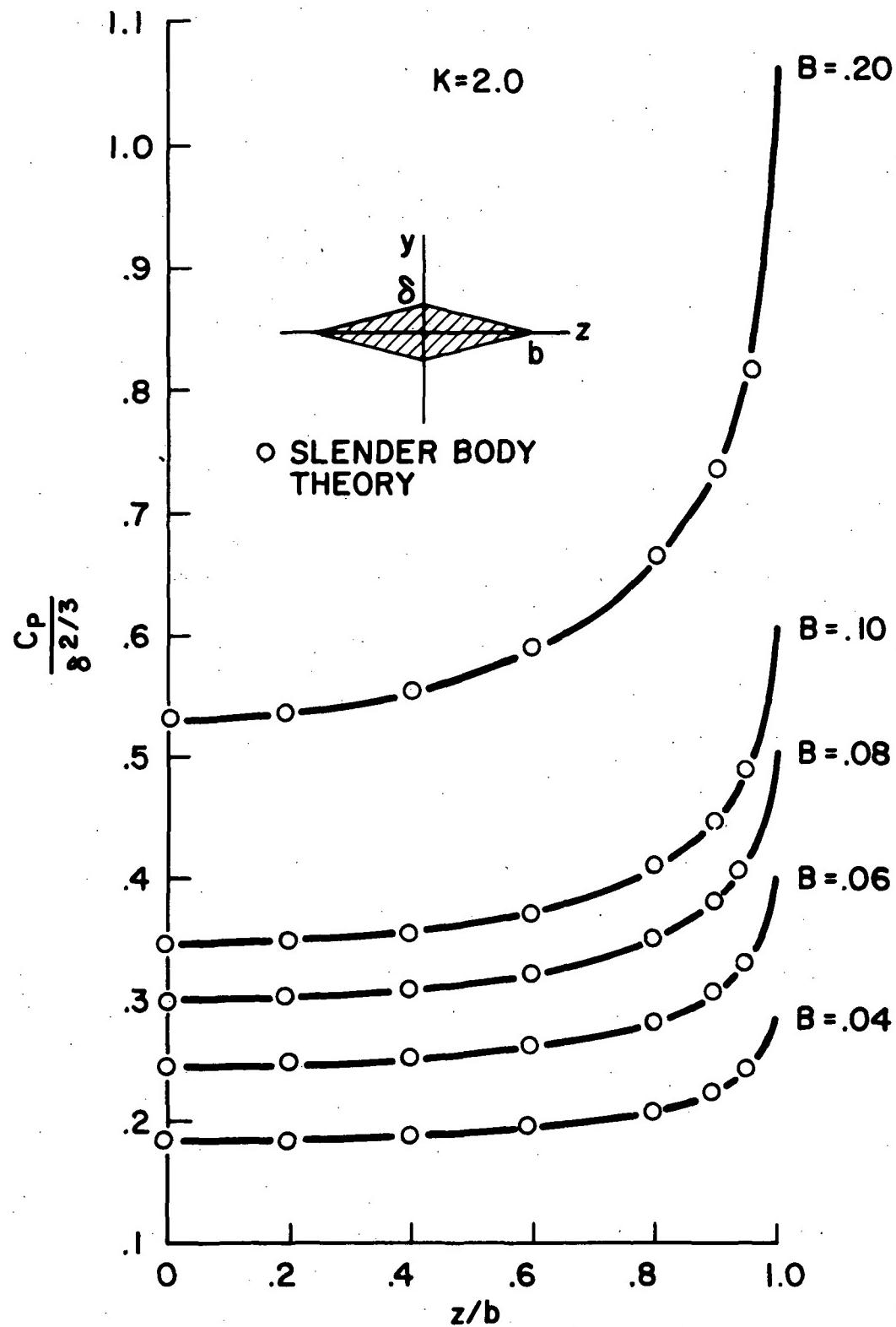
Figure 4.3. Pressure Distributions on the Surface of a Rhombic Wing for K = 2.0.

49
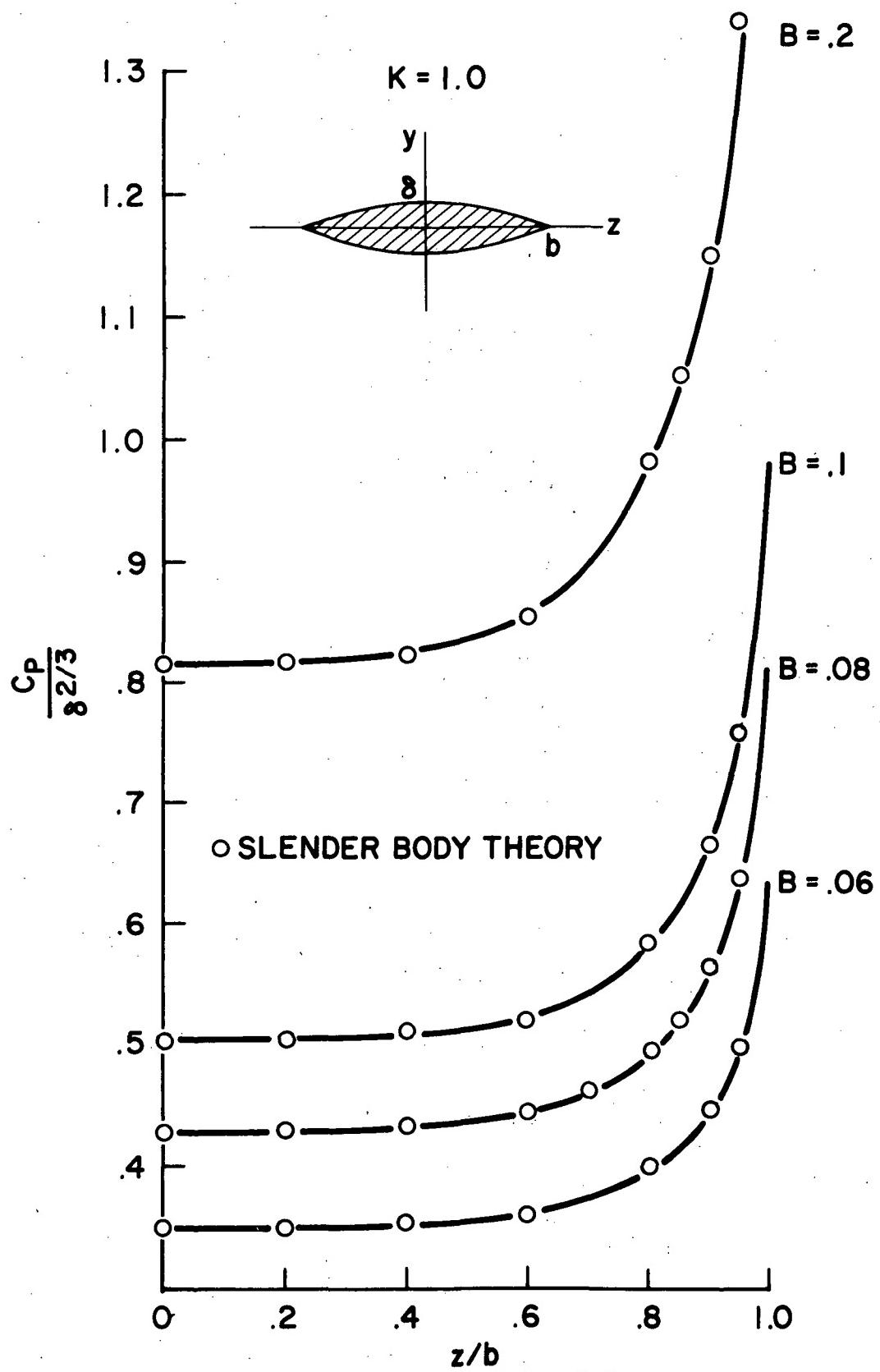
Figure 4.4. Pressure Distributions on the Surface of a Circular Wing for K = 1.0.

50
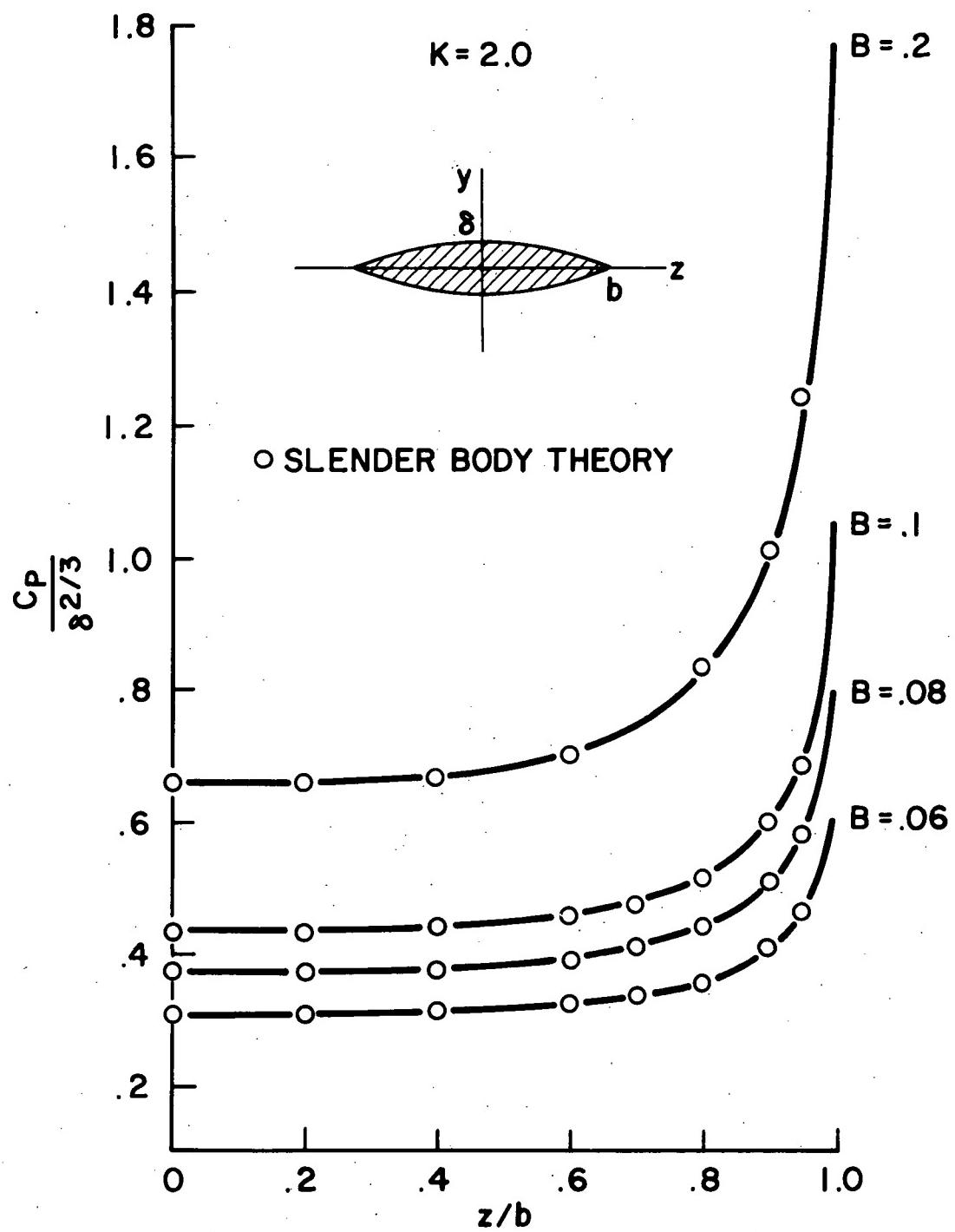
Figure 4.5. Pressure Distributions on the Surface of a Circular Wing for K = 2.0.
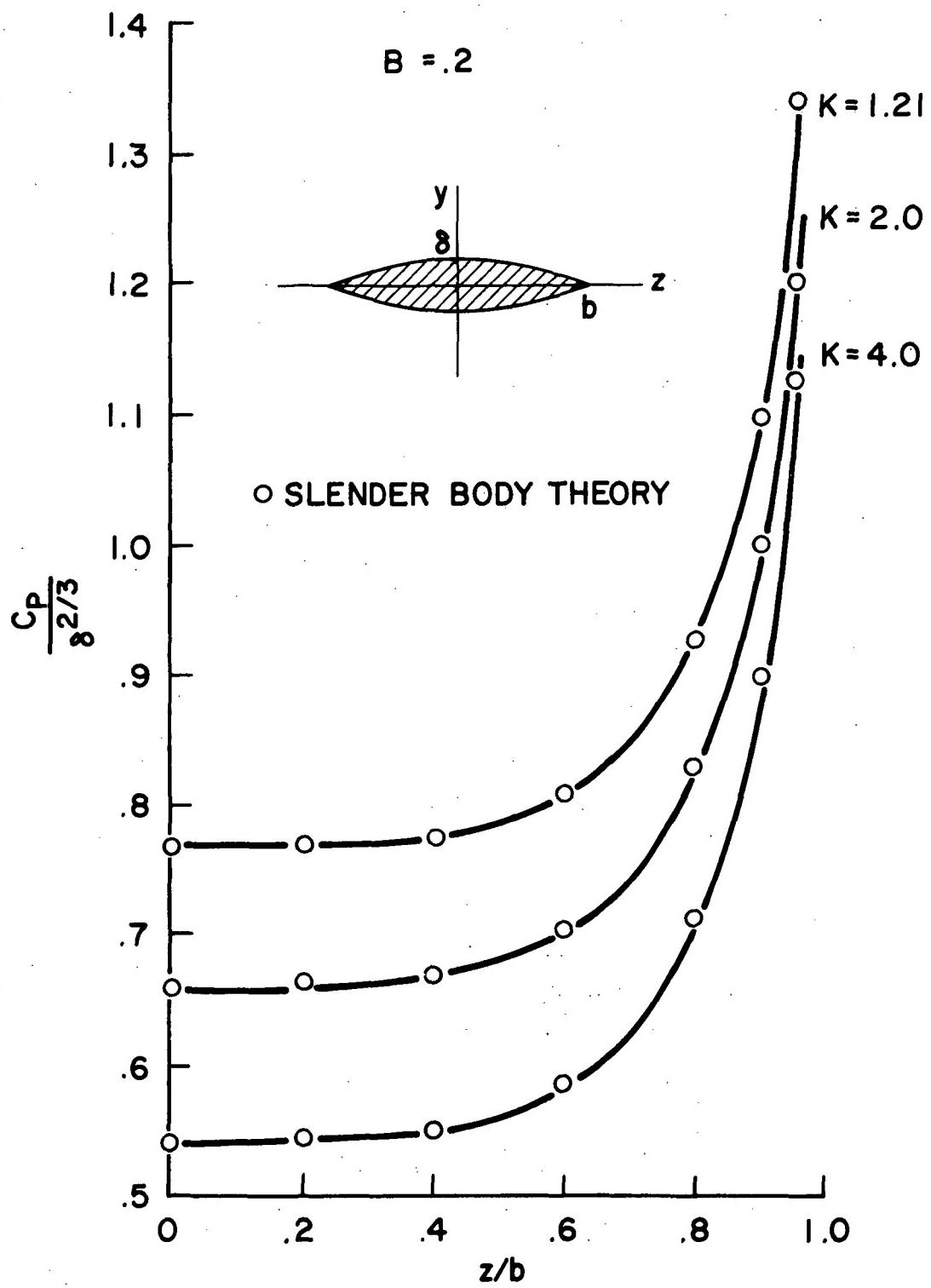
Figure 4.6. Pressure Distributions on the Surface of a Circular Wing for B = .2.
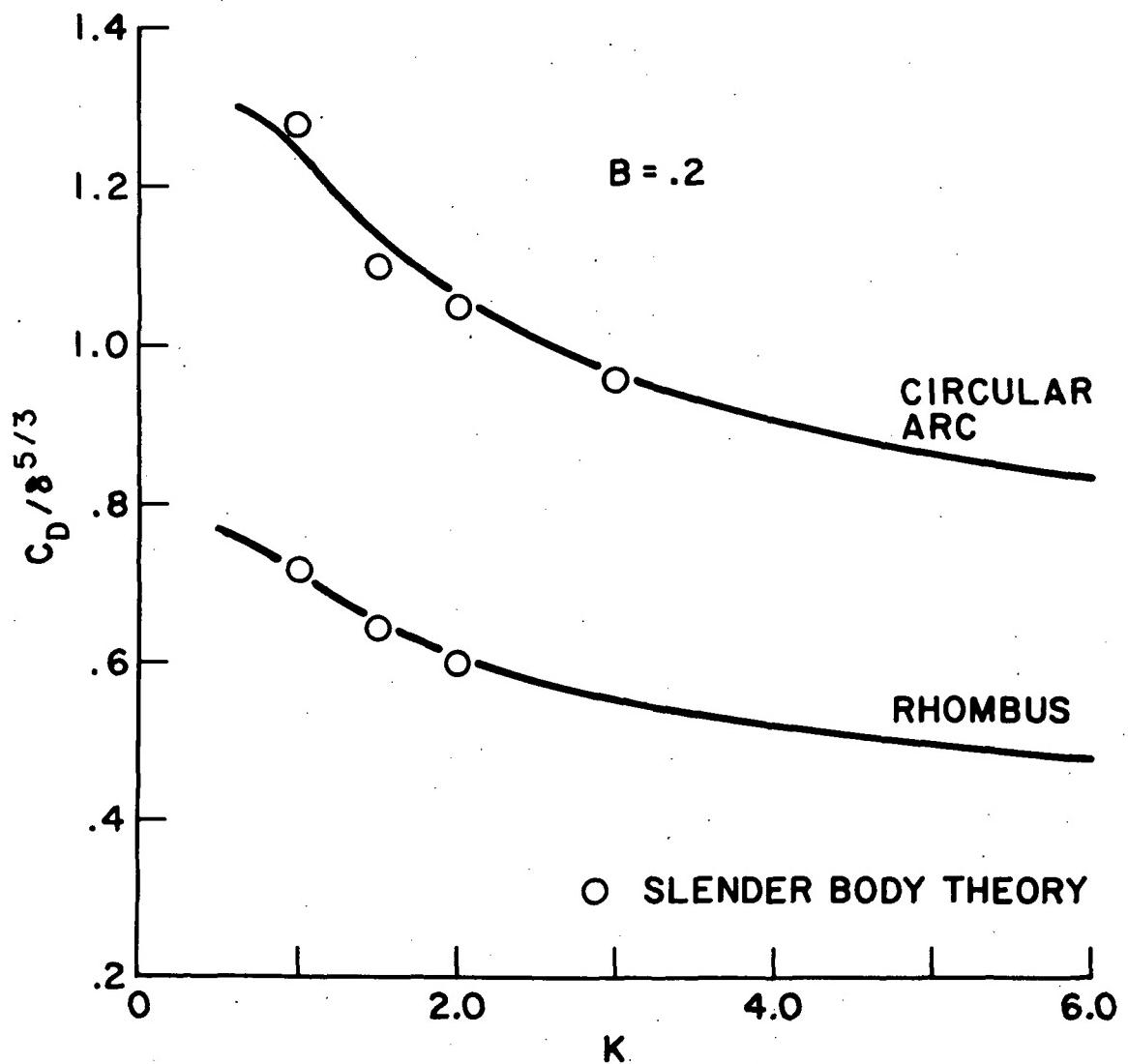
Figure 4.7. Drag Coefficients for Rhombic and Circular Wings for B = .2.

Page Intentionally Left Blank

CHAPTER 5

CONCLUDING REMARKS

The method presented in this dissertation falls in the general category of shock fitting techniques. It is simpler than conventional methods mainly because the state on one side of the shock is known. The results of the computations indicate that, generally the method has a wide range of applicability. The limitation of the algorithm is best expressed in terms of the location of the shock wave, i.e. it must not fall on the wing.

For wings which have rounded tips, such as conical wings of elliptic cross section, the same algorithm can be used provided that the numerical solution is modified in the neighborhood of the tip in order to recover the correct singularity. The conical solution in the neighborhood of a rounded tip is given by the solution, in the hodograph plane, of two dimensional transonic flow towards that tip.

The agreement between slender body theory and the numerical calculations indicates the usefulness of equations (4.14) - (4.17), (II-5) and (II-6). These equations are applicable for values of K_e for which $C_1(K_e)$ has a similarity form. Expressed in terms of the similarity parameters B and K, $C_1(K_e)$ possesses such a form if $B \leq .20$ and $K \leq 2.0$.

It should be noted that the wing shapes considered are given by the family of curves $F(Z) = 1 - Z^n$, n = 1, 2, 3, 4 which have different area distributions along the Z axis. Also, the function $C_1(K_e)$ does not seem to be particularly partial to any of these shapes.

The computer program has been written to ease the understanding of the logic rather than optimizing it for computing speed.

There are many areas in which future work would be beneficial. One would be to extend this method to lifting wings. In particular conical wings with arbitrary afterbodies could be studied. This can be done by extending the solution from the conical region to the region over the afterbody using the method of characteristics.

BIBLIOGRAPHY

1. Newman, P.A. and D.O. Allison. "Annoted Bibliography on Transonic Flow Theory," NASA Langley Working Paper, LWP-942, Hampton, Virginia, 1971.

2. Cole, J.D. "Twenty Years of Transonic Flow," Boeing Scientific Research Laboratories, Document D1-82-0878, Seattle, Washington, 1969.

3. Garabedian, P.R. and D.G. Korn. "Numerical Design of Transonic Airfoils," in Numerical Solution of Partial Differential Equation-II, Academic Press, 1971.

4. Magnus, R. and H. Yoshihara. "Inviscid Transonic Flow Over Airfoils," AIAA Paper, No.70-47, 1970.

5. Murman, E.M. and J.D. Cole. "Calculations of Plane Steady Transonic Flows," AIAA J., Vol.9, No.1, pp.114-121, January 1971.

6. Krupp, J.A. and E.M. Murman. "The Numerical Calculation of Steady Transonic Flows Past Thin Lifting Airfoils and Slender Bodies," AIAA Paper, No.71-566, 1971.

7. Krupp, J.A. "The Numerical Calculation of Plane Steady Transonic Flows Past Thin Lifting Airfoils," Boeing Scientific Research Laboratories, Document D180-12958-1, Seattle, Washington, 1971

8. Ballhaus W.F. and F.R. Bailey. "Numerical Calculation of Transonic Flow About Swept Wings," AIAA Paper, No.72-677, 1972.

9. Cole, J.D. and A.F. Messeter. "Expansion Procedures and Similarity Laws for Transonic Flow," Office of Scientific Research, Technical Note 56-1, Guggenheim Aeronautical Laboratory, Pasadena, 1956.

10. Cole, J.D. Perturbation Methods in Applied Mathematics, Ginn Blaisdell, Waltham, Massachusetts, 1968.

11. Isaacson, E. and H.B. Keller. Analysis of Numerical Methods, John Wiley & Sons, New York, 1966.

12. Messiter, A.F. Expansion Procedures and Similarity Laws for Transonic Flow, Ph.D. in Aeronautics, Guggenheim Aeronautical Laboratory, Pasadena, 1957.

13. Kopal, Z. Tables of Supersonic Flows Around Cones, Department of Electrical Engineering, Center of Analysis, M.I.T., Cambridge, Massachusetts, 1947.

14. Shen, Y-c. "Similarity Solution for Transonic Flow Past a Cone,"
     Office of Scientific Research, Technical Note 56-121, Guggenheim
     Aeronautical Laboratory, Pasadena, 1956.

15. Frankl, F.I. and E.A. Karpovich. Gas Dynamics of Thin Bodies,
     Interscience, London, England, 1953 (Translated by M.D. Friedman).

16. Hovanessian, S.A. and L.A. Pipes. Digital Computer Methods in
     Engineering, McGraw-Hill, New York, 1969.

17. Liepman, H.W. and A. Roshko. Elements of Gasdynamics, John Wiley
     & Sons, New York, 1957.

18. Mitchell, A.R. Methods in Partial Differential Equations, John
     Wiley & Sons, New York, 1969.

19. Tychanov, A.N. and A.A. Samarski. Partial Differential Equations
     of Mathematical Physics, Vol.1, Holden-Day, San Francisco,
     California, 1964.

APPENDIX I

PROGRAM LISTING

The computer program used in this dissertation was written in Fortran IV for an IBM 360/91. The main program is included here for reference.

The following subprograms are called by the main program:

INTERP   Computes interpolated values for the potential

OUTPUT   Prints out values of the potential

SLEND   Computes values of the pressure coefficient using slender wing theory.

```
      IMPLICIT REAL*8(A-H,O-Z)
      DIMENSION CMAX(20,20),C(40,20),A4(40,20),A5(40,20),A6(40,20),
     1A7(40,20),P(40,20),DJ(40,20)
      DIMENSION PC(20),PCA(20),A0(4),A1(20),A2(20),A3(20),DC(20)
      DIMENSION PPR(20),JPR(20),CA(20),PCS(20),CN(20),A(20)
      DIMENSION PP(40),PM(40)
      DIMENSION PH(20),CP(20)
      DIMENSION F9A(20), R(20),A8(20),ZC(20)
      DO 4000 MM=1,13
      READ(5,4001) TK,B,CMAX1
 4001 FORMAT(3F15.7)
      WRITE(6,1001)
 1001 FORMAT(1H1)
      WRITE(6,3)TK,B
    3 FORMAT(10X,'K = ',F8.4,10X,'B = ',F8.4)
      LMAX=12
      CONS=.0001
      NMAX=200
      W=1.93
      IM, =40
      JM, =20
      IMA1=IMAX-1
      AMAX=1.5707963
      DBS=1./R**2
      CVERGE=.000025
      DVERGE=100.
      DO 4 J=1,JMAX
      JPR(J)=J
    4 CONTINUE
      DO 5 J=1,JMAX
      CMAX(J,1)=CMAX1
    5 CONTINUE
      DA=AMAX/JMAX
      DDA=1./DA
      DDAS=1./(DA*DA)
      T2=DFLOAT(JMAX)
      DO 10 J=1,JMAX
      T1=DFLOAT(J-1)
      A(J)=DA/2.+AMAX*T1/T2
```

```
10 CONTINUE
   DO 20 J=1,JMAX
   PC(J)=B*DSIN(A(J))
20 CONTINUE

   AO(1)=.5*DA
   AO(2)=DA
   AO(3)=AMAX-.5*DA
   AO(4)=AMAX-DA

   DO 30 J=1,4
   PCA(J)=B*DCOS(A(J))
30 CONTINUE

   DO 35 I=1,IMAX
   DO 35 J=1,JMAX
   P(I,J)=0.
35 CONTINUE

   DO 40 J=1,JMAX
   A1(J)=DSIN(A(J))*DCOS(A(J))
   A2(J)=A1(J)**2
   A3(J)=DCOS(A(J))**2-DSIN(A(J))**2
40 CONTINUE

   DO 1000 L=1,LMAX

   T1=DFLOAT(IMAX)
   DO 60 J=1,JMAX
   DC(J)=CMAX(J,L)/(T1-.5)
   DO 50 I=1,IMAX
   T2=DFLOAT(I)
   C(I,J)=DC(J)*(T2-.5)
50 CONTINUE
60 CONTINUE

   DO 70 J=1,JMAX
   DO 80 I=1,IMAX
   IC=C(I,J)
   A4(I,J)=DSINH(TC)*DCOSH(TC)
   A5(I,J)=A4(I,J)*A4(I,J)
   A6(I,J)=DSINH(TC)**2+DCOSH(TC)**2
   A7(I,J)=A1(J)*A4(I,J)**2.
80 CONTINUE
70 CONTINUE

   DJ(I,J)   IS ONE OVER THE JACOBIAN
```

61

```
      DO 90 J=1,JMAX
      DO 100 I=1,IMAX
      TC=C(I,J)
      DJ(I,J)=1./(DSINH(TC)**2+DSIN(A(J))**2)
100   CONTINUE
90    CONTINUE

      DO 500 N=1,NMAX
      I=0
      J=0
      RES=0.
150   CONTINUE
      J=J+1

      IF(L.EQ.1) GO TO 155
      CALL INTERP(J,JMAX,IMAX,IMAX1,C,DC,P,PP,PM)
155   CONTINUE

160   CONTINUE
      I=I+1

      IF(L.NE.1) GO TO 156
      IF(J.EQ.JMAX) GO TO 158
      PP(I)=P(I,J+1)
      IF(I.EQ.1) GO TO 157
      PP(I-1)=P(I-1,J+1)
157   CONTINUE
      PP(I+1)=P(I+1,J+1)
158   CONTINUE
      IF(J.EQ.1) GO TO 159
      PM(I)=P(I,J-1)
      IF(I.EQ.1) GO TO 161
      PM(I-1)=P(I-1,J-1)
161   CONTINUE
      PM(I+1)=P(I+1,J-1)
159   CONTINUE
156   CONTINUE
      B1=DJ(I,J)*A5(I,J)
      B2=DJ(I,J)*A7(I,J)
      B3=DJ(I,J)*A2(J)
      B4=A4(I,J)*(2.*DJ(I,J)**2*(A5(I,J)-A2(J))+1.-DJ(I,J)*A6(I,J))
      B5= A1(J)*(2.*DJ(I,J)**2*(A5(I,J)-A2(J))+1.+DJ(I,J)*A3(J))

      IF(I.EQ.1) GO TO 200
      IF(J.EQ.1) GO TO 230
      IF(J.EQ.JMAX) GO TO 240
```

```
      DDC=1./(DC(J))
      DDCS=1./(DC(J)*DC(J))
      TLT=TK+2.4*(P(I,J)-DJ(I,J)*(.5*A4(I,J)*(P(I+1,J)-P(I-1,J))/DC(J))
     1-.5*A1(J)*(PP(I)-PM(I))/DA))
      C1=TLT*B1-DBS
      C2=TLT*B2
      C3=TLT*B3-DBS
      C4=TLT*B4
      C5=TLT*B5
      D1=.5/(C1*DDCS+C3*DDAS)
      PCC=DDCS*(P(I+1,J)+P(I-1,J))
      PCA1=.25*DDA*DDC*(PP(I+1)-PM(I+1)-PP(I-1)+PM(I-1))
      PAA=DDAS*(PP(I)+PM(I))
      PC1=.5*DDC*(P(I+1,J)-P(I-1,J))
      PA=.5*DDA*(PP(I)-PM(I))
      GO TO 400
  200 IF(J.EQ.1) GO TO 250
      IF(J.EQ.JMAX) GO TO 260
      DDC=1./(DC(J))
      DDCS=1./(DC(J)*DC(J))
      TLT=TK+2.4*(P(I,J)-DJ(I,J)*(.5*A4(I,J)*(P(I+1,J)-P(I,J))/DC(J)
     1+PC(J))-.5*A1(J)*(PP(I)-PM(I))/DA))
      C1=TLT*B1-DBS
      C2=TLT*B2
      C3=TLT*B3-DBS
      C4=TLT*B4
      C5=TLT*B5
      D1=1./(C1*DDCS+2.*C3*DDAS-.5*C4*DDC)
      PCC=P(I+1,J)*DDCS-PC(J)*DDC
      PCA1=.25*DDA*(PP(I+1)-PP(I+1)+PC(J+1)-PC(J-1)-PM(I+1)-PM(
     1I))/DC(J-1))
      PAA=DDAS*(PP(I)+PM(I))
      PC1=.5*P(I+1,J)*DDC+.5*PC(J)
      PA=.5*DDA*(PP(I)-PM(I))
      GO TO 400
  230 CONTINUE
      DDC=1./(DC(J))
      DDCS=1./(DC(J)*DC(J))
      TLT=TK+2.4*(P(I,J)-DJ(I,J)*(.5*A4(I,J)*(P(I+1,J)-P(I-1,J))/DC(J))
     1-.5*A1(J)*(PP(I)-PM(I))/DA))
      C1=TLT*B1-DBS
      C2=TLT*B2
      C3=TLT*B3-DBS
      C4=TLT*B4
```

63

```
C5=TLT*B5
D1=1./(2.*C1*DDCS+C3*DDAS+.5*C5*DDA)
PCC=DDCS*(P(I+1,J)+P(I-1,J))
PCA1=.25*DDA*DDC*(PP(I+1,J)-P(I+1,J)-PP(I-1,J)+P(I-1,J))
PAA=DDAS*PP(I)
PC1=.5*DDC*(P(I+1,J)-P(I-1,J))
PA=.5*DDA*PP(I)

        GO TO 400
240 CONTINUE

DDC=1./(DC(J))
DDCS=1./(DC(J)*DC(J))
TLT=TK+2.4*(P(I,J)-DJ(I,J)*(.5*A4(I,J)*(P(I+1,J)-P(I-1,J))/DC(J)
1-.5*A1(J)*(P(I,J)-PM(I))/DA))
C1=TLT*B1-DBS
C2=TLT*B2
C3=TLT*B3-DBS
C4=TLT*B4
C5=TLT*B5
D1=1./(2.*C1*DDCS+C3*DDAS-.5*C5*DDA)
.PCC=DDCS*(P(I+1,J)+P(I-1,J))
PCA1=.25*DDA*DDC*(P(I+1,J)-PM(I+1,J)-P(I-1,J)+PM(I-1))
PAA=DDAS*PM(I)
PC1=.5*DDC*(P(I+1,J)-P(I-1,J))
PA=-.5*DDA*PM(I)

        GO TO 400
250 CONTINUE

DDC=1./(DC(J))
DDCS=1./(DC(J)*DC(J))
TLT=TK+2.4*(P(I,J)-DJ(I,J)*(.5*A4(I,J)*((P(I+1,J)-P(I,J))/DC(J)
1+PC(J))-.5*A1(J)*(PP(I)-P(I,J))/DA))
C1=TLT*B1-DBS
C2=TLT*B2
C3=TLT*B3-DBS
C4=TLT*B4
C5=TLT*B5
D1=1./(C1*DDCS+C2*DDA*DDC/16.+C3*DDAS-.5*C4*DDC+.5*C5*DDA)
PCC=P(I+1,J)*DDCS-PC(J)*DDC
PCA1=.25*PCA(1)+.125*PCA(2)+(PP(I+1)-P(I+1,J)-PP(I))*DDC*DDA/16.
PAA=DDAS*PP(I)
PC1=.5*P(I+1,J)*DDC+.5*PC(J)
PA=.5*DDA*PP(I)

        GO TO 490
```

```
260 CONTINUE
    DDC=1./(DC(J))
    DDCS=1./(DC(J)*DC(J))
    TLT=TK+2.4*(P(I,J)-DJ(I,J))*(.5*A4(I,J)*((P(I+1,J)-P(I,J))/DC(J)
   1+P(C(J))-.5*A1(J)*(P(I,J)-PM(I))/DA))
    C1=TLT*B1-DAS
    C2=TLT*B2
    C3=TLT*B3-DBS
    C4=TLT*B4
    C5=TLT*B5
    D1=1./(C1*DDCS-C2*DDA*DDC/16.+C3*DDAS-.5*C4*DDC-.5*C5*DDA)
    PCC=P(I+1,J)*DDCS-PC(J)*DDC
    PCA1=.25*PCA(3)+.125*PCA(4)+DDA*DDC*(P(I+1,J)+PM(I)-PM(I+1))/16.
    PAA=DDAS*PM(I)
    PC1=.5*P(I+1,J)*DDC+.5*PC(J)
    PA=-.5*DDA*PM(I)

400 CONTINUE
    C6=.25*C2**2-C1*C3
    IF(C6.GT.0.) GO TO 2002
    GO TO 2004
2002 WRITE(6,2003)I,J,N,C6,B1,H2,B3,C1,C2,C3,TLT
2003 FORMAT(3I4,8F12.5)
    GO TO 3000
2004 CONTINUE
    PNEW=D1*(C1*PCC-C2*PCA1+C3*PAA-C4*PC1+C5*PA)
    POLD=P(I,J)
    P(I,J)=W*PNEW+(1.-W)*P(I,J)
    DP=DABS(P(I,J)-POLD)
    RES=DMAX1(RES,DP)
    IF(I.LT.IMAX1) GO TO 150
    I=0
    IF(J.LT.JMAX) GO TO 150
    IF(RES.LT.CVERGE) GO TO 600
    IF(RES.GT.DVERGE) GO TO 601
500 CONTINUE
600 CONTINUE

    CALL OUTPUT(IMAX,JPR,P)

    CA(J) IS DC/DA

    IF(L.EQ.1) GO TO 700
    GO TO 702
700 DO 701 J=1,JMAX
    CA(J)=0.
701 CONTINUE
```

65

```
      GO TO 704
  702 DO 703 J=1,JMAX
      IF(J.EQ.1) CA(J)=.5*DDA*(CMAX(J+1,L  )-CMAX(J,L  ))
      IF(J.EQ.1) GO TO 705
      IF(J.EQ.JMAX) CA(J)=.5*DDA*(CMAX(J,L  )-CMAX(J-1,L  ))
      IF(J.EQ.JMAX) GO TO 705
      CA(J)=.5*DDA*(CMAX(J+1,L  )-CMAX(J-1,L  ))
  705 CONTINUE
  703 CONTINUE
  704 CONTINUE

      PCS(J) IS DP/DC  AT THE SHOCK

      I=IMAX
      DO 706 J=1,JMAX
      PCS(J)=.5*(P(I-2,J)-4.*P(I-1,J))/DC(J)
  706 CONTINUE

      CN(J) IS THE VALUE OF SH(C)CH(C)

      LL=L+1
      RESS=0.
      DO 707 J=1,JMAX
      F1=1.2*DJ(IMAX,J)*PCS(J)*(A4(IMAX,J)+A1(J)*CA(J))**3/TK-CA(J)*
     1A7(IMAX,J)-A2(J)*CA(J)**2
      F2=(1.+CA(J)**2)/(TK*B**2)
      F4=CMAX(J,L)
      F3=DCOS(A(J))**2*DSINH(F4)**2+DSIN(A(J))**2*DCOSH(F4)**2
      F5=F1+F2*F3
      CN(J)=DSQRT(F5)
      F6=(2.*CN(J))**2+1.
      F7=2.*CN(J)+DSQRT(F6)
      F9=.5*DLOG(F7)
      F9A(J)=F9
      DPSS=DABS(F4-F9)
      RESS=DMAX1(RESS,DPSS)
      CMAX(J,LL)=F9
      RS=(DSIN(A(J))*DSINH(F9))**2+(DCOS(A(J))*DCOSH(F9))**2
      R(J)=DSQRT(RS)
  707 CONTINUE
      IF(RESS.LT.CONS) GO TO 3000
 1000 CONTINUE
 3000 CONTINUE
      WRITE(6,709)L
  709 FORMAT(1H0,'L = ',I4)
```

66

```
      WRITE(6,1002)
1002  FORMAT(1H0)
      DO 710 J=1,JMAX
      WRITE(6,1300) A(J)
      WRITE(6,1300) CA(J),F9A(J),R(J)
1300  FORMAT(8F15.7)
710   CONTINUE

      PB IS THE VALUE OF THE POTENTIAL ON THE BODY

      WRITE(6,1001)
      DO 800 J=1,JMAX
      PB(J)=P(1,J)-.5*(P(2,J)-P(1,J))+3.*(P(1,J)-2.*P(2,J)+P(3,J))/8.
      WRITE(6,1300) PB(J)
800   CONTINUE

      CP IS THE PRESSURE COEFFICIENT

      WRITE(6,1002)
      DO 851 J=1,JMAX
      DTANA=1./DTAN(A(J))
      IF(J.EQ.1) CP(J)=PB(J)+.5*DTANA*(-3.*PB(J)+4.*PB(J+1)-PB(J+2))*DDA
      IF(J.EQ.1) GO TO 850
      IF(J.EQ.JMAX) CP(J)=PB(J)+.5*DTANA*(3.*PB(J)-4.*PB(J-1)+PB(J-2))*
     1DDA
      IF(J.EQ.JMAX) GO TO 850
      CP(J)=PB(J)+.5*DTANA*(PB(J+1)-PB(J-1))*DDA
850   CONTINUE
      ZC(J)=DCOS(A(J))
      CP(J)=-2.*CP(J)
      WRITE(6,1300) CP(J),ZC(J)
851   CONTINUE

      SUM=-4.*(1.570796  -A(JMAX))*PB(JMAX)*DSIN(A(JMAX))
      JMM=JMAX-1
      DO 900 J=6,JMM
      SUM=SUM+2.*(PB(J)*DSIN(A(J))+PB(J+1)*DSIN(A(J+1)))*(A(J)-A(J+1))
900   CONTINUE
      WRITE(6,1002)
      WRITE(6,899) SUM
899   FORMAT(1H0,' DRAG = ',F15.7)
```

```
      CPM=CP(JMAX)
      CALL  SLEND(TK,B,CPM)

      GO TO 603
  601 WRITE(6,602)
  602 FORMAT(' THE SOLUTION DIVERGED')
  603 CONTINUE
 4000 CONTINUE
      STOP
      END
```

APPENDIX II

In this appendix two more nonlifting conical wings will be considered and the function $C_1(K_e)$ will be calculated using the matching method described in Section 4.2.

In terms of conical variables the first is described by the cubic function

$$F(Z) = 1 - Z^3 \qquad\qquad 0 \le Z \le 1 \qquad\qquad (II.1)$$

which in the physical coordinates corresponds to

$$y = \delta x \left(1 - \frac{z^3}{b^3 x^3} \right) \qquad\qquad (II.2)$$

and the second by the quartic function

$$F(Z) = 1 - Z^4 \qquad\qquad 0 \le Z \le 1 \qquad\qquad (II.3)$$

which corresponds to

$$y = \delta x \left(1 - \frac{z^4}{b^4 x^4} \right) \qquad\qquad (II.4)$$

Formulas for pressure distributions on slender wings can now be obtained using equations (4.2), (4.8) and (4.11). The constant of proportionality k, obtained using equation (4.2), is equal to $\frac{3}{\pi}$ for the cubic and $\frac{16}{5\pi}$ for the quartic. Performing the integration in equation (4.11) and the differentiation in equation (4.8) gives

$$\frac{C_p}{\delta^{2/3}} = -\frac{3}{\pi} B \left\{ \log \frac{3}{\pi} + 3 \log B + \frac{2}{3} Z + 2Z^3 + \frac{2}{3} \log (1-Z^2) \right.$$
$$\left. + \frac{1}{3} \log \frac{(1-Z)}{(1+Z)} + Z^4 \log \frac{(1-Z)}{(1+Z)} - \frac{4}{3} + 2C_1(K_e) \right\} \qquad (II.5)$$

for the cubic and

$$\frac{C_p}{\delta^{2/3}} = -\frac{16}{5\pi} B \left\{ \log \frac{16}{5\pi} + 3 \log B + \frac{19}{12} Z^2 + 3Z^4 + \log (1-Z^2) \right.$$
$$\left. + \frac{1}{2} Z^5 \log \frac{(1-Z)}{(1+Z)} - \frac{7}{5} + 2C_1(K_e) \right\} \qquad (II.6)$$

for the quartic.

The values of the function $C_1(K_e)$ obtained by matching equations (II.5) and (II.6) with the pressure coefficients obtained numerically are shown in Figure 4.1.